

**Full-Scale Snow Load Simulations on a Fabric Covered  
Steel Arch Structure**

By

Andrew Gies, P.Eng

A thesis submitted to the Faculty of Graduate Studies of  
The University of Manitoba

In partial fulfillment of the requirements of the degree of

MASTER OF SCIENCE

Department of Biosystems Engineering

University of Manitoba

Winnipeg

Copyright © 2007 by Andrew Gies, P.Eng

**THE UNIVERSITY OF MANITOBA**  
**FACULTY OF GRADUATE STUDIES**  
\*\*\*\*\*  
**COPYRIGHT PERMISSION**

**Full-Scale Snow Load Simulations on a Fabric Covered Steel Arch Structure**

**BY**

**Andrew Gies, P. Eng**

**A Thesis/Practicum submitted to the Faculty of Graduate Studies of The University of  
Manitoba in partial fulfillment of the requirement of the degree**

**MASTER OF SCIENCE**

**Andrew Gies, P. Eng © 2007**

**Permission has been granted to the University of Manitoba Libraries to lend a copy of this thesis/practicum, to Library and Archives Canada (LAC) to lend a copy of this thesis/practicum, and to LAC's agent (UMI/ProQuest) to microfilm, sell copies and to publish an abstract of this thesis/practicum.**

**This reproduction or copy of this thesis has been made available by authority of the copyright owner solely for the purpose of private study and research, and may only be reproduced and copied as permitted by copyright laws or with express written authorization from the copyright owner.**

## Table of Contents

Table of Contents.....	2
Acknowledgements.....	4
Abstract.....	5
List of Figures.....	6
List of Tables.....	8
1 Introduction.....	9
2 Background Review.....	10
2.1 Testing Approach.....	16
3 Materials and Methods.....	19
3.1 Materials.....	19
3.1.1 Experimental setup.....	19
3.1.2 Tensioned fabric structure.....	19
3.1.3 Steel.....	21
3.1.4 Canvas.....	21
3.1.5 Data acquisition system.....	22
3.1.6 Draw-Wire Displacement Sensors.....	22
3.1.7 DC Power Supply.....	23
3.1.8 Data Acquisition Unit.....	24
3.1.9 Multi Chambered Water Storage System.....	25
3.2 Methods.....	27
3.2.1 Draw-wire Displacement Sensor Calibration.....	27
3.2.2 Draw-wire Displacement Sensor Measurement Points.....	28
3.2.3 Test 1: Bags over arch.....	32
3.2.4 Test 2: Bags beside arch.....	36
3.2.5 Test 3: Barrels under arch.....	38
4 Results.....	42
4.1 Results from Bags over Arch Test.....	42
4.2 Results from Bags Beside Arch Test.....	44
4.3 Results from Barrels Under Arch Test.....	47
5 Discussion.....	50
5.1 Vertical Deflection.....	50
5.1.1 Discussion Bags over Arch Test.....	51
5.1.2 Discussion Bags Beside Arch Test.....	52
5.1.3 Discussion Barrels Under Arch Test.....	54

5.1.4	Computer Aided Modeling Analysis Discussion.....	55
5.2	Horizontal Deflection.....	59
5.3	Co-efficient of Lateral Stability .....	61
6	Conclusion .....	64
7	Recommendations for further study.....	67
8	References.....	68
9	Bibliography .....	69
10	Appendix.....	71

## **Acknowledgements**

I would like to acknowledge several people for their contributions to this research:

- My advisor Dr. Kris Dick, P. Eng for providing insight, wisdom and guidance throughout this process.
- Allan Aikins, Len Peters and Joe Kuffner of HiQual Engineered Buildings, for providing financial and material support for this project.
- Matt McDonald, technician, for providing assistance with setting up the data acquisition system used during this research.
- Thesis committee members Dr. M.G. (Ron) Britton P.Eng, and Dr. James Blatz P.Eng.

Finally I would like to acknowledge the Natural Sciences and Engineering Research Council of Canada for providing financial support for this research under the Industrial Post Graduate Scholarship program.

## **Abstract**

This study investigated the behavior of a full-scale fabric covered steel arch structure under simulated snow load conditions, and assessed the interaction between the tensioned-fabric membrane and the steel arches in the overall building structural system. The principal objectives of the study were to evaluate the changes in deflection of a main arch structural member in the building when subjected to simulated loads with and without a tensioned fabric membrane, and from this evaluation, to establish a co-efficient that relates the behaviour of the interaction between the steel-arch and the tensioned fabric membrane. Three test procedures were conducted to induce a deflection in a test-arch section by positioning the simulated load directly on top, beside, and below the test arch section. The data recorded from the test procedures showed a maximum deflection at the peak of the arch as 19.5 mm for the Bags Over Arch test, 21.2 mm for the Bags Beside Arch test, and 22.4 mm for the Barrels Under Arch test.

When using the Barrels Under Arch test deflections as a basis for comparison, the co-efficient of lateral stability was determined to be 0.95 and 0.87 at the peak of test arch section when comparing the results against the Bags Over Arch and Bags Beside Arch test procedures respectively. When comparing the results for the deflection at the peak of the arch from the Barrels Under Arch test against a similarly loaded computer model, a co-efficient of lateral stability was determined to be 0.35. This co-efficient could only be inferred, as the deflection value for one set of the comparable data is based on simulated and not experimentally derived data.

## List of Figures

Figure 1:	Anticlastic surface.....	14
Figure 2:	Typical arch structures anticlastic surface .....	14
Figure 3:	rendering of the PQ3045 manufactured by HiQual .....	20
Figure 4:	the central manifold system, showing the individual hoses and valves for each chamber, and the volumetric flow meter .....	26
Figure 5:	Calibration curve for sensor 107, the 500mm displacement sensor measuring the vertical deflection for the peak of the test arch section.....	28
Figure 6:	Deflection measurement locations on the test arch member .....	29
Figure 7:	Data acquisition system, test arch section and steel frame .....	31
Figure 8:	Position of the MCEWSS with respect to the test arch section .....	33
Figure 9:	Position of the MCWSS with respect to the test arch section - Test 2 .....	36
Figure 10:	Barrels attached to the underside of the test arch section .....	39
Figure 11:	Position and spacing of barrels during testing .....	39
Figure 12:	The average vertical deflection for each monitored location on the test arch at the trial start, trial full load, and load release as measured throughout each trial. Bags Over Arch (Gies, 2007) .....	43
Figure 13:	The average vertical deflection for each monitored location on the test arch at the trial start, trial full load, and load release as measured throughout each trial. Bags Beside Arch (Gies, 2007) .....	45
Figure 14:	The average vertical deflection for each monitored location on the test arch at the trial start, trial full load, and load release as measured throughout each trial. Barrels Under Arch (Gies, 2007).....	48
Figure 15:	The deflection during Bags Over Arch test averaged over 3 trials for vertical displacement sensors 104, 107 and 109 on the test arch at the trial start, trial full load, and load release (Gies, 2007) .....	51
Figure 16:	The deflection during Bags Beside Arch test averaged over 3 trials for vertical displacement sensors 104, 107 and 109 on the test arch at the trial start, trial full load, and load release (Gies, 2007).....	52
Figure 17:	The deflection during Barrels Under Arch test averaged over 3 trials for vertical displacement sensors 104, 107 and 109 on the test arch at the trial start, trial full load, and load release (Gies, 2007).....	54
Figure 18:	Simulated test arch section analysed by RISA-3D (Gies 2007) .....	56
Figure 19:	The average deflection over all tests for horizontal displacement sensor 105 at the trial start, trial full load, and load release (Gies, 2007).....	60

Figure 20: The average deflection over all tests for horizontal displacement sensor 110 at the trial start, trial full load, and load release (Gies, 2007)..... 60

## List of Tables

Table 1:	The average vertical deflection for sensors 104, 107 and 109 on the test arch as measured throughout each trial. Bags over Arch (Gies, 2007) .....	43
Table 2:	The average horizontal deflection for each displacement sensor on the test arch as measured throughout each trial. Bags Over Arch (Gies, 2007).....	44
Table 3:	The average vertical deflection for sensors 104, 107 and 109 on the test arch as measured throughout each trial. Bags Beside Arch (Gies, 2007).....	46
Table 4:	The average horizontal deflection for each displacement sensor on the test arch as measured throughout each trial. Bags Beside Arch (Gies, 2007)....	46
Table 5:	The average vertical deflection for sensors 104, 107 and 109 on the test arch as measured throughout each trial. Barrels Under Arch (Gies, 2007).....	48
Table 6:	The average horizontal deflection for each displacement sensor on the test arch as measured throughout each trial. Barrels Under Arch (Gies, 2007) .	49
Table 7:	The average vertical deflection for computer model nodes N13, N16 and N19 on the simulated test arch as analysed and predicted by RISA-3D. ....	57
Table 8:	A comparison of the average maximum vertical deflections recorded during the test procedures and with those predicted by Risa3D (Gies, 2007) .....	58
Table 9:	Co-efficient of lateral stability based on the barrels under arch test results (Gies, 2007).....	62
Table 10:	Co-efficient of lateral stability using the barrels under arch test and the RISA3D software peak of arch deflection data. ....	63

## 1 INTRODUCTION

Fabric covered arch buildings are becoming more common on the Canadian landscape. These buildings consist of a series of steel arch members that are covered with a tensioned fabric membrane that forms the roof and walls of the building. They provide a relatively inexpensive and efficient way for industrial and agricultural users to obtain effective shelters. The widespread use of these buildings includes a variety of applications from machine storage and industrial fabrication shops to livestock rearing purposes.

The design of fabric covered arch buildings presents some unique challenges for engineers when compared with more traditional building types. One of these challenges is designing the structure for the Canadian climate and the snow that can accumulate throughout the winter season. The current National Building Code does not provide guidance to the engineer for tensioned fabric membranes. As a result, the structural analysis of these buildings involves a number of design assumptions for building cladding. This experimental study investigates the behavior of a full-scale fabric covered steel arch structure under simulated snow loading conditions. The interaction between the tensioned-fabric membrane and the steel arches in the overall building structural system was studied to establish a co-efficient that relates interaction between the steel-arch and tensioned fabric membrane.

The determination of how the tensioned fabric membrane may contribute as a co-efficient of lateral stability will enable the engineer to better understand how the tensioned fabric membrane interacts with the overall building structure.

## 2 BACKGROUND REVIEW

Trebilcock (2004) describes tensioned fabric structures (TFS) as those structures where the “structural concept is explicit in the architecture” or shape of the completed building. The term explicit refers to the nakedness of the completed structure. The fabric is stretched taut and thin over a building, and does not hide any of the structural elements from anyone who cares to look. With a TFS what you see is what you get, all of the structural intricacies are not hidden behind walls or the ceiling, and everything is there in plain view, explicit, leaving nothing to the imagination.

The use of fabric as a structural element is not a new phenomenon. Indeed, as Shaeffer (1996) explains, this technology has been used by civilizations for basic shelter for more than 40,000 years, initially using animal skins as the outer membrane. Modern TFS should not be confused with tents or any other basic flexible membrane-over-frame buildings that have existed throughout the years. Schierle (1968) describes TFS as a relative new comer in the structural world, with the first tensioned fabric membranes designed for use on buildings beginning in the early 1950’s. Tents are simply a frame with a fabric covering draped over without precision, and secured to the ground. Tents are portable, temporary and not intended to be a permanent fixture at any point in their useful life. TFS share the same basic ingredients as tents, namely a frame and fabric membrane, but this is where the similarities end. Where a tent is imprecise, the TFS is a building designed from the ground up. Careful thought goes into how the building will react to all loading conditions it will be expected to encounter over its lifetime. Where a tent is temporary, a TFS is designed to be more permanent.

This TFS building type employs an internal structural framework or skeleton over which the fabric membrane is pre-stressed to form the complete building enclosure. Specifically, this report will study a building where tubular steel arches form the internal framework of the TFS. These arches serve two important purposes. They provide a physical mechanism for applying the tension in the outer fabric membrane and the arch frames collect and resolve the tension forces from the membrane to the foundation of the building.

The arch is an effective and efficient shape to use for TFS. The curved surface allows for the outer membrane to be supported along its entire contact surface, and results with the arch supports having direct influence over the geometric shape of the building. This follows the explicit structural concept as defined by Trebilcock (2004). Arches are convex shapes that are designed to resist compression, while being capable of resisting the bending moments introduced by an unbalanced loading situation. Trebilcock (2004) states that the arch shape is further enhanced when its structural members are constructed using tubular steel due to the tubular sections inherent ability to resist buckling, increasing the underlying lateral strength of the structure.

How is it that a membrane surface with little or no resistance to either bending or shear stresses can be used to safely enclose a building, and provide resistance to both internal and external loading? A simple explanation of the load bearing characteristics of the TFS is provided by Huntington (2004) using a synonym for the tensioned membrane surface. Huntington (2004) likens the membrane of a TFS to a grid of individual threads. A single thread when pulled taut has considerable strength in tension, but has little to no resistance to compression or bending forces. Even when these individual threads are

Tents allow their outer fabric membranes to flutter about in the wind, and flex greatly under applied loads. TFS membranes are designed to remain in static equilibrium, the outer membranes remaining taut and relatively unmoving under any expected loading condition. This tautness or tension is what makes the TFS unique, and tents simply a fabric structure.

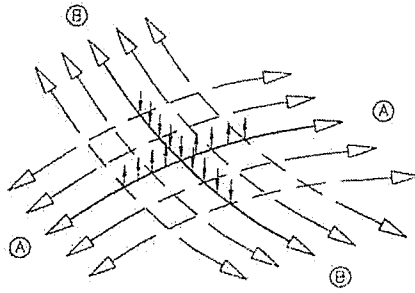
The outer membrane of a TFS is kept taut to resist the design loads of the building in its particular location. Valerio (1985) provides that the tension within the membrane ensures a static equilibrium of the building system under the design loads of the building. The tension is applied to the membrane by the application of either internal or external forces. External forces refer to membranes where the tension is applied by pressurized air. Internal forces refer to membranes tensioned and supported by physical and mechanical means, most commonly cables, posts and arches.

Leonard (1988) describes two broad classes of TFS, the first is a structure supported by uniaxially stressed members, or cable structures, and the second are those structures supported by biaxially stressed members, or membrane structures. This report will be limited to membrane structures that Leonard (1988) further breaks down into 4 separate categories. These four categories are comprised of: air supported structures, structures supported with inflated or pressurized structural members, pre-stressed membrane structures, and hybrid structures employing both pre-stressed membranes and structural elements. Pre-stressed membrane structures are what best describes the TFS that will be studied in this report, namely the fabric covered arch buildings that are manufactured by HiQual Engineered Structures.

woven together to form a fabric, the resistance to any force besides tension is negligible. It is the curvature of the tensioned membrane surface that provides the resistance to loads acting in all directions.

When properly constructed, TFS are capable of maintaining their shape both when subjected to loads pushing down on the surface of the membrane (e.g. Snow loads) and when subjected to loads pushing the membrane from the inside (e.g. Wind loads). The complete rigidity of the membrane and its ability to maintain its shape is a result of the shape of the tensioned surface. The tensioned surface forms a shape known as an anticlastic shape. Refer to figure 1 and figure 2 on page 13 for diagrams of typical anticlastic surfaces.

Valerio (1985) defines anticlastic as a surface that is doubly curved, with the principle axes curving in opposite directions, while Schierle (1968) describes it as a curved surface in which the main curvatures are in mutually opposed directions. Other descriptions of membranes that refer to an anticlastic shaped surface are saddle, hyperboloid and antisphere. No matter what the surface is called, Huntington (2004) states that the anticlastic shape is the method in which the tensioned membrane is able to resist loads and carry them to supporting members in pure tension. Huntington (2004) goes further to explain that on the anticlastic surface, the fibres with convex curvature increase tension to resist upward loads, while the fibres with concave curvature increase tension to resist the downward loads.



(ABOVE) On an anticlastic surface, fibers with convex curvature, A, increase their tension to resist upward loads, while those with concave curvature, B, increase their tension to resist downward loads.

Figure 1: Anticlastic surface.  
(Huntington, 2004)

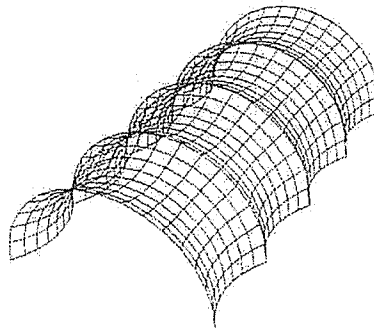
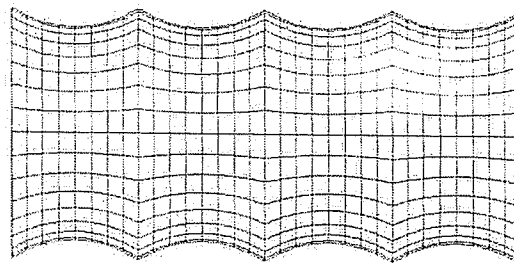


Figure 2: Typical arch structures anticlastic surface  
(Valerio, 1985)

The term tension as it pertains to TFS implies a structure that is wholly dependent on tension to support both the building weight and any applied loads. However, no structural system can be completely dependent on tension and hope to remain standing, as any downward pressures that are applied to the structure must be resisted by some type of compression members. This remains true for TFS. The membrane is tensioned throughout its surface, but all forces that it experiences from wind, snow and other loading conditions are resolved by the underlying structural skeleton, and the foundation of the building.

TFS offers several advantages over conventional building types (Schaeffer, 1996):

1. High span to weight ratios. When used for spans from 60 to 180 feet, TFS offer high cost advantages over conventional building types.
2. High build quality. The majority of components used to construct TFS are factory built, allowing for strict quality control and large production runs.
3. Low installation costs. Installation is made quickly by the use of relatively lightweight components that are factory built and require little on site fabrication and labour as the building is erected.
4. High safety rating. In the event of a collapse in the outer membrane, the structural skeleton will remain intact. The lightweight nature of the membrane material ensures that any collapse of the building membrane will not be a catastrophic failure.
5. High applied load to self-weight ratio when compared to conventional buildings.

## 2.1 Testing Approach

The main goal of this research is to record the deflection of a full-scale fabric covered steel arch structure under simulated snow loading conditions, and to assess the resulting data to determine the interaction between the tensioned-fabric cover and the steel arches while the load is applied. The principal objectives of these tests were:

- 1) to evaluate the changes in deflection of a main arch structural member in the building when subjected to simulated loads with and without a tensioned fabric membrane;
- 2) to establish a co-efficient that relates the behaviour of the interaction between the steel-arch and tensioned fabric membrane.

The tests were conducted in September 2005 on a full-scale fabric covered steel arch structure measuring 30-foot wide by 60-feet long by 15-foot high. This building was formed using a series of tubular structural arch members positioned at 5-foot intervals, laterally braced with a system of purlins, and finished with vertical end walls. To the structural skeleton of the interconnected steel arches, the roof and walls of the building were created by a fabric membrane that is positioned over top of the building skeleton and tensioned along the base of the end walls and sides of the building.

To conduct the tests, it was necessary to choose a structural arch member located near the centre of the building to be used as the test arch. The centre of the building was chosen to conduct the testing to minimise the effects of the end-walls of the building, where additional lateral bracing supports the arch members for wind resistance. This centre test arch was used exclusively throughout each trial as loads were applied and removed to determine the deflection. The deflection of the test arch was measured during

each test in both the horizontal (x) and vertical (y) directions using a series of extensometers positioned along the test arch at regular intervals. Deformation of the test arch was determined by recording the change of the resistance inside each extensometer and in turn, the resulting voltage output. This change in voltage is proportional to the instantaneous deformation of the test arch at each extensometer location, and was collected at 15 second intervals at each location separately using a data acquisition system.

To determine the interaction between the test arch and the tensioned fabric membrane, a series of trials were conducted that varied the way in which the load was applied to the building. It was decided that there would be three different methods used for the application of the load to the building, and three separate trials completed for each load application method.

To simulate a snow load condition on the outer membrane of the building, a load was applied using a “saddle bag” system that utilized a series of water filled chambers extending along the effective width of the arch roof surface. The effective width of the arch was determined based on the slope of the roof and dictated in the National Building Code of Canada – NBCC-1995, the code that was in use at the time of testing in September 2005. Each chamber of the saddle bag system was filled with an equal amount of water with the purpose of inducing a measurable deflection of a main arch structural member.

The first load application method tested the interaction of the test arch and tensioned fabric membrane by applying the load centered directly over top of the test arch and the tensioned fabric membrane.

The second load application method tested the tensioned fabric membrane without the direct interaction of the test arch by applying the load directly overtop of the 5-foot wide section of fabric immediately adjacent to the test arch.

The third load application method tested the test arch without the direct interaction of the tensioned fabric membrane by applying the load beneath the test arch, essentially pulling it downwards from the interior of the building.

Following the completion of the trials for each load application method, the test arch deflection data from each separate trial were downloaded from the data acquisition system for analysis. The various data points were organized to observe the deflection distance for each trial, and to determine any trends in the data that would aid in the understanding of the interaction between the test arch and the tensioned fabric membrane.

### **3 MATERIALS AND METHODS**

This research test program recorded the deflection of a steel arch section under three separate loading conditions devised to stress the arch in a similar way to a snow loading condition. Each load condition was tested in three separate trials, for a total of nine trials.

#### **3.1 Materials**

##### **3.1.1 Experimental setup**

The trials were conducted using a steel arch section within a 30-foot diameter arch tensioned fabric structure that was 45 feet in length. A steel arch section towards the centre of this structure was chosen to use as the test section. A series of draw-wire displacement sensors were affixed to the test section at regular intervals to measure the deflection along the entire length of the arch. The sensors were physically attached to a data acquisition system that recorded the arch deflection throughout each trial.

##### **3.1.2 Tensioned fabric structure**

The building used for this test series was a HiQual Engineered Structures tensioned fabric structure model PQ3045. Refer to figure 3 for a rendering of the PQ3045. This structure is described as a “portable quonset building” and has a semi-circular arch shape. A system of tubular steel arch members spaced 5-feet apart, form the major framework of the building. The arches give the building a true semi circular shape, with a diameter of 30 feet, and therefore a height of 15 feet at the peak of the structure. This structure is 45-feet long, and consists of a total of 10 main arch sections that frame into a tubular steel base frame system. The base frame system is constructed of tubular

steel, and provides a continuous base frame along the entire perimeter of the structure. The entire framework of the building consisting of the main arch sections and base frame are anchored to the ground using a series of 16, 32-inch long screw-type anchors.

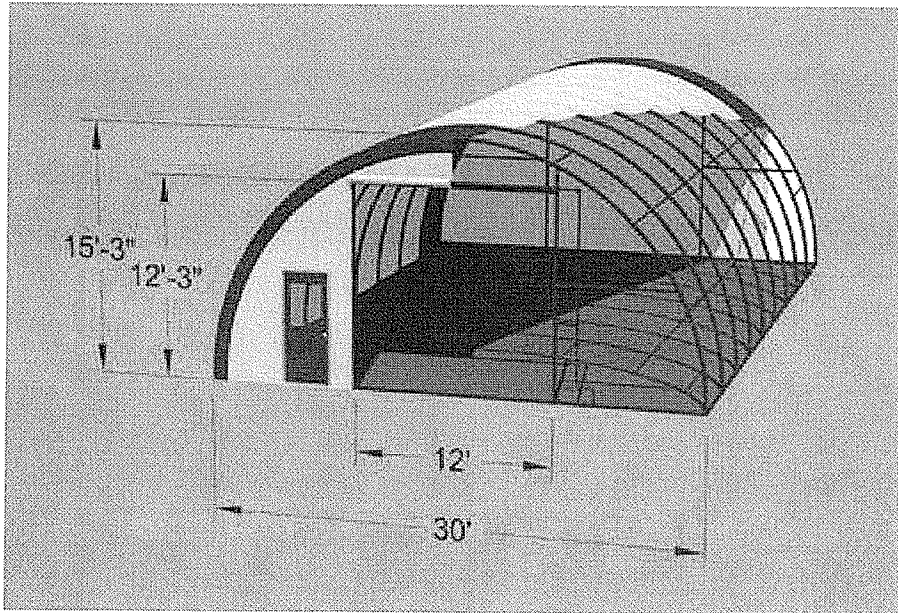


Figure 3: rendering of the PQ3045 manufactured by HiQual (HiQual Engineered Structures, 2007)

The building is enclosed with a tensioned fabric canvas that covers the entire length of the building, and includes separate tensioned fabric canvas sections for both of the buildings end walls. Along the base of canvas where it meets the base-frame of the building, there is a pocket sewn into the canvas in which a length of steel tube is inserted. The function of the steel tube is to apply the tension to the canvas shell on the building using a series of ratchet-strap winches placed at the base of each main arch section.

### 3.1.3 Steel

The main arch members and base frame of the PQ3045 are constructed of 3" O.D. round x .100 wall tube ASTM A500-03 grade B.

The properties of this steel are listed below:

Yield Strength:	350 MPa
Ultimate Strength:	450 MPa

### 3.1.4 Canvas

The canvas used for the tensioned fabric shell of the structure is made from 4-mil Nova-shield II RU88x-6 material. The yarn used to weave this canvas is made from a high-density polyethylene (HDPE) polymer. The properties of the canvas are listed below: (Nova-Shield II, 2006)

Scrim weight:	219 gram per square metre
Coating thickness:	102 microns per side
Total Thickness:	0.59 millimetres
Final Coated Weight:	407 gram per square metre
Strip Tensile:	2275 Newton per 50 millimetre strip
Mullen Burst:	4588 kPa
Light Transmission:	12.0%
Light Reflection:	74.5%
Light Absorption:	13.7%
Operating Temperature:	-60 to 70 Celsius
UV Resistance:	>90%

### 3.1.5 Data acquisition system

A computer-based data acquisition system was set up to measure and collect the deflections that occurred in the arch section throughout each of the nine trials. The system consisted of four major components; 13 draw-wire displacement sensors, a multi-channel data acquisition unit, a DC voltage power supply, and a computer that collected and stored the data for each trial. The data acquisition system was set to capture the data from each displacement sensor at 15-second intervals throughout the trial. Data collection was initiated manually prior to the beginning of the trial, and stopped manually following the completion of each trial.

### 3.1.6 Draw-Wire Displacement Sensors

The arch deflection throughout the trials was measured using 13 separate Micro-Epsilon Minter Draw-wire Displacement Sensors. These 13 sensors consisted of 4 model WPS-250-MK30-P with a 250mm-displacement range, 5 WPS-500-MK30-P with a 500 mm displacement range, and 4 WPS-750-MK30-P with a 750mm-displacement range.

Draw-wire displacement sensors are capable of measuring linear translation by the use of a proportion output voltage signal. A flexible draw-wire that is constructed of stainless steel is wound around a spring loaded wire drum. An input voltage is applied to the sensor, and as the draw-wire is extended or retracted from the wire drum, the resistance inside the sensors internal potentiometer changes, altering the output voltage of the sensor. The change in output voltage changes linearly with respect to the distance that the draw-wire is extended or retracted from the wire-drum. This output voltage is recorded at set time intervals, and is used to capture the linear deflection of the surface

that the draw-wire is attached.

The specifications of the sensors are listed below (Micro-Epsilon, 2004):

Signal Output:	Potentiometer
Measuring range:	250mm (WPS-250) 500mm (WPS-500) 750mm (WPS-750)
Linearity:	+/- 0.1% of full scale
Resolution:	quasi infinite
Sensor:	wire/hybrid-potentiometer
Temperature Range:	-20 to 80 Celsius
Housing Material:	Aluminium
Draw-wire Material:	coated polyimid stainless steel
Wire Retraction Force:	1 Newton
Wire Extension Force:	2.5 Newton

### 3.1.7 DC Power Supply

An external DC power supply was used to provide excitation voltage to each of the 13 draw wire displacement sensors. The voltage supplied to the sensors in the data acquisition system was maintained at 10.0V DC throughout all trials and the pre and post calibration of the sensors. As the wires within the draw wire displacement sensors were extended or retracted, the output voltage from each sensor would change from the original 10V excitation voltage. It was this change in voltage from which displacement in the arch section was determined.

The specifications of the DC power supply are listed below:

Anatek Electronics Ltd. Regulated DC power supply

Output: 0-25 VDC

0-2 A

Input: 117 VAC

60 Hz

8A

### 3.1.8 Data Acquisition Unit

An Agilent 34970A Data Acquisition Unit was used throughout all trials and pre and post calibration to read the output from the draw-wire displacement sensors. The data acquisition unit was physically wired to each of the 13 draw-wire displacement sensors and the DC power supply. The unit measured the real-time voltage being outputted through each sensor, and was programmed to measure and download this voltage information to the computer for storage at regular 15-second intervals. In addition to this sensor data, the unit measured and downloaded the level of excitation voltage from the power supply.

The data acquisition unit was connected directly to software on a PC that was used to store the data from each trial. The program used by the PC to read and download the information from the data acquisition unit was Agilent Benchlink Data Logger 3 software.

### 3.1.9 Multi Chambered Water Storage System

To apply a load on the test arch during two of the three loading conditions, a custom-built multi-chambered water storage system was draped over the outside of the structure, over top of the test arch section. This storage system was designed to apply a uniform load across the effective length of the test arch section, over its entire 5-foot wide tributary area. The storage system comprised of 24 identical and individual chambers that could be filled or drained through central access points in each chamber. Each chamber measured 18 by 60 inches in area, and between each chamber was a strip of separating material 2 inches in width. The final shape of the storage system was formed by positioning the 24 chambers side by side that resulted in overall dimensions of 60 inches wide and 38 feet long.

The water storage system was constructed using the same 4-mil Nova-shield II RU88x-6 material that was used to construct the canvas for the test structure. The only difference being that the water storage system material was brown in colour, while the building canvas was white.

Attached to each of the 24 individual access points, an identical ½ inch common garden water hose 50 feet in length was connected. The free end of each of these hoses was identified with a number, and then attached to a central manifold system that provided the water flow to and from each chamber. Figure 4 on page 25 shows a picture of the central manifold system used during the trials.

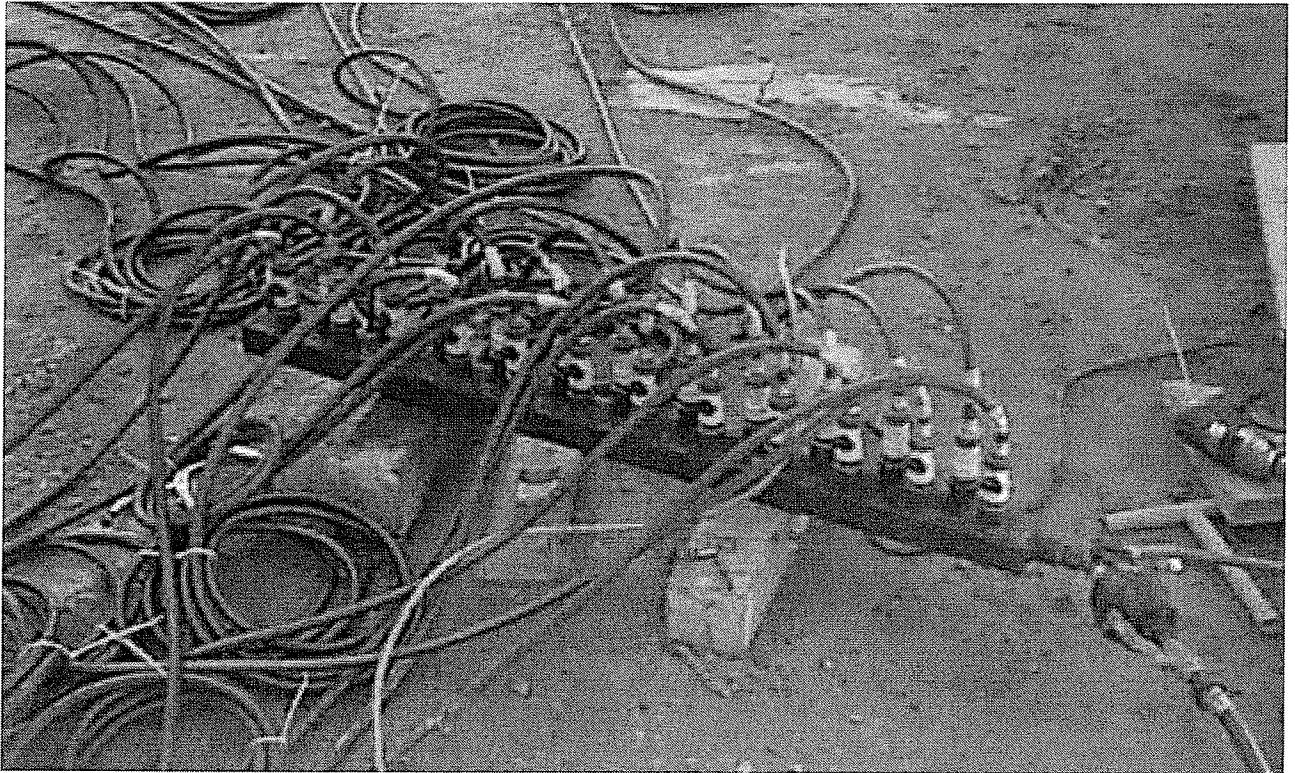


Figure 4: the central manifold system, showing the individual hoses and valves for each chamber, and the volumetric flow meter (Gies, 2005)

At the manifold, each hose was equipped with an individual valve that allowed the chambers to be filled and drained separately. The water supply to the storage system was attached to a separate inlet point at the base of the manifold. At this inlet point, the water passed through an inline volumetric water meter to allow for precise filling of each individual water chamber. The volumetric water meter used for the trials was a Kent US Gallon meter, model 10522538.

## 3.2 Methods

### 3.2.1 Draw-wire Displacement Sensor Calibration

The draw-wire displacement sensors were individually calibrated prior to the commencement of the trials. Following the completion of all the trials, the calibration of each individual sensor was verified. This pre and post calibration ensured that the sensors were operating properly and accurately throughout all trials.

The calibration process extended and retracted the draw-wire displacement sensors throughout a pre-defined range, while the output from the sensors was recorded by the data acquisition system. The data acquisition system used for the calibration of the sensors was identical to the system used throughout all the experimental trials.

To extend and retract the sensors for the calibration procedure, a computer controlled universal testing machine was used to provide a precise movement. The machine used for this project was an ATS Series 1410 Computer Controlled Universal Testing Machine, with a 10 000 pound (44.48kN) capacity.

The 750mm sensors were extended and retracted to a distance of 688mm, in distance intervals of 140mm. The 500mm sensors were extended and retracted to a distance of 450mm, in distance intervals of 90mm. The 250mm sensors were extended and retracted through a distance of 200mm, in distance intervals of 40mm.

At each distance interval, the voltage output from the respective sensor was recorded manually and by the data acquisition unit. Following the completion of the calibration procedure, the voltages and the corresponding distance intervals were plotted using a spreadsheet program. Linear regression analysis was performed for each data set to obtain a calibration curve. With the slope of this line, it is possible to convert the

outputted voltage from each sensor into a distance in millimetres. The following chart shows the calibration curve for sensor 107, the 500mm displacement sensor measuring the vertical deflection for the peak of the test arch section.

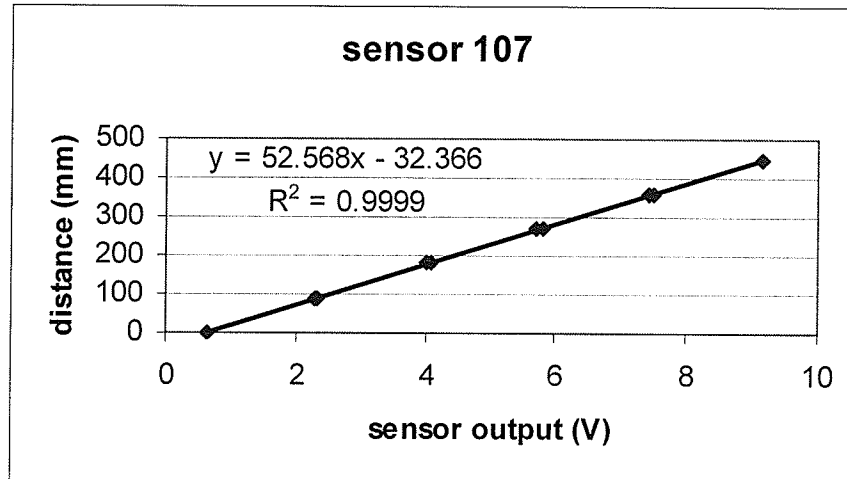


Figure 5: Calibration curve for sensor 107, the 500mm displacement sensor measuring the vertical deflection for the peak of the test arch section. (Gies, 2007)

The calibration curves and all data collected (by the unit) are contained in Appendix A.

### 3.2.2 Draw-wire Displacement Sensor Measurement Points

A total of 13 draw-wire displacement sensors were used to measure the deflection of the arch in each of the 9 trials.

A series of 11 locations along the length of the test arch section was used to measure vertical deflection. These locations were started with a point at the peak of the test arch section, and continued for five (5) points on both sides of the peak at 2-foot intervals. In addition to the 11 points used for measuring vertical deflection, two (2)

additional points were used to measure the horizontal or out-of-plane deflection of the test arch section. These two additional points were located 4-feet on either side of the peak of the test arch section. Figure 6 shows a diagram of the location of all the measurement points on the test arch.

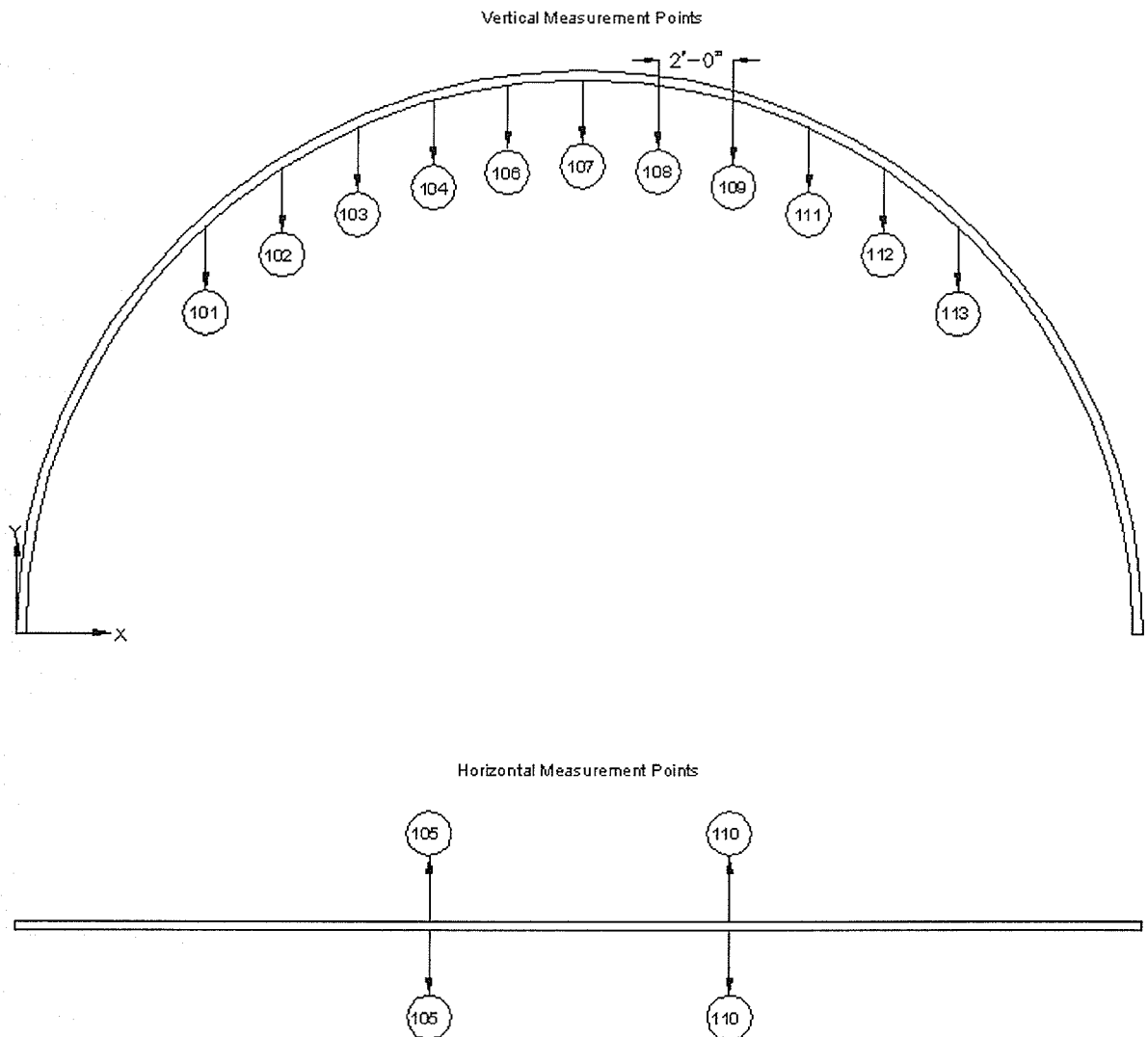


Figure 6: Deflection measurement locations on the test arch member  
(Gies, 2007)

The data acquisition system used for the trials was located a safe distance away from the area in which the testing was being conducted. All of the draw-wire displacement sensors were positioned next to the data acquisition system. Each sensor was required to be physically attached to points on the arch in order for the movement of the arch to cause the draw-wire to extend or retract, and result in a deflection value being measured.

Each of the draw-wire sensors had a clip attached to the free end of the retractable wire. To physically attach the sensors retractable wire to the various measuring points on the test arch section, a length of braided fishing line was used. Braided fishing string was chosen because of its high strength, small diameter, and its resistance to linear deformation. A separate length of string was used to attach each measuring point on the test arch section to its respective draw-wire sensor clip.

To ensure that the vertical measurement points captured only vertical deflections in the arch, and the horizontal measurements captured only horizontal deflections, a standalone steel frame was designed and built.

- 1) This frame provided a platform that was used to ensure that the strings were guided in the correct direction required for each point, (horizontally or vertically)
- 2) The frame served to change the direction of the string towards to the data acquisition system.

The string for the vertical measurement points was pulled straight down to the framework through individual pulleys that guided the string in the direction of the data acquisition system. The string for the horizontal measurement points was first pulled perpendicular to the arch for approximately 1-foot, before being passed through a pulley

that guided the string vertically down and finally through an additional pulley that guided the string in the direction of the data acquisition system. Pulleys were used in the frame to minimize friction resistance on the string as the test arch deflected throughout each trial.

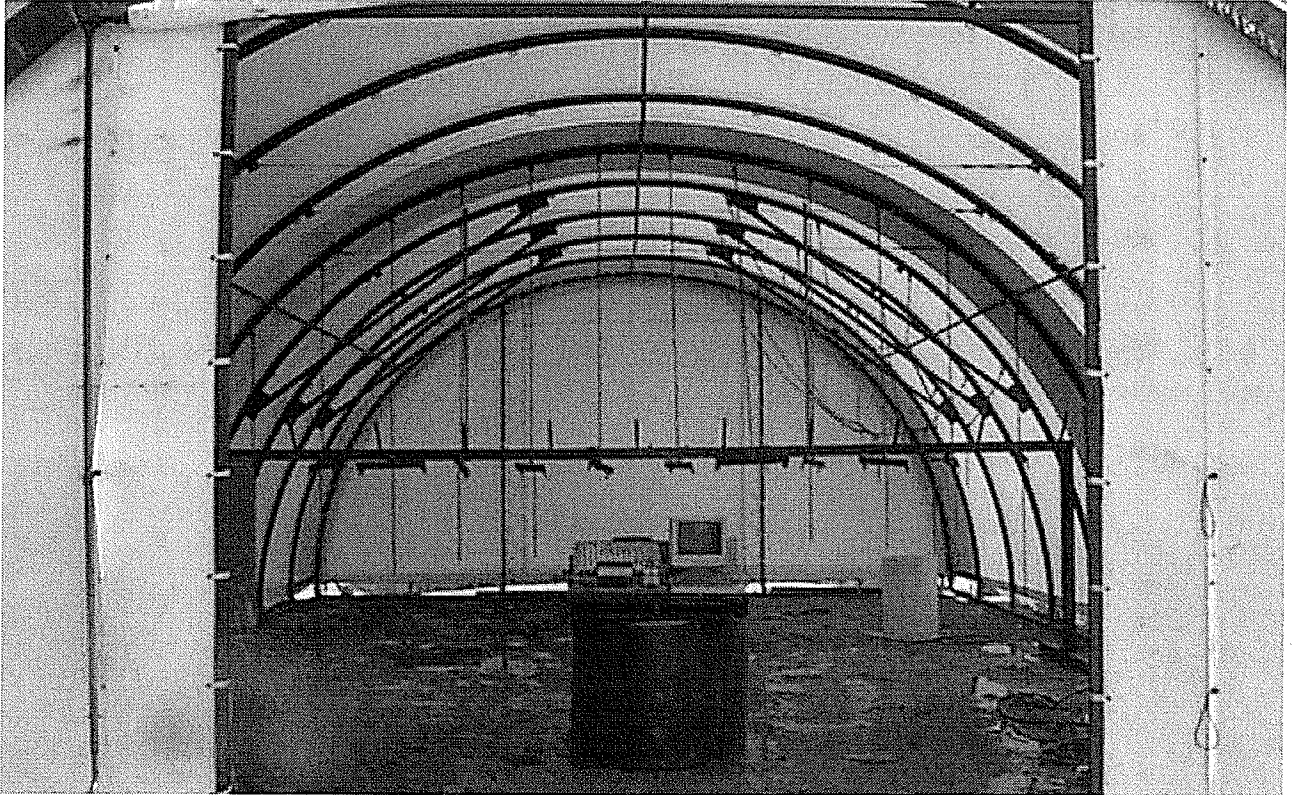


Figure 7: Data acquisition system, test arch section and steel frame  
(Gies, 2005)

After the clip at the end of the draw wire sensors and the respective measuring point on the test arch were connected with the string, it was necessary to extend each draw-wire to approximately the mid point of its displacement range. This was done because as the arch was forced to deflect downwards, and then retract back when the load was removed during each trial, there needed to be a range of displacement available for each sensor to retract or extend its draw-wire, and measure the change in voltage. With

each draw-wire sensor extended to approximately the mid-point of its displacement, the string connecting it to the test arch was pulled taut to allow the setup to remain in a static condition.

This static condition was recorded by the voltage reading of each sensor. The deflection of the each measuring point on the test arch was measured against the static condition of the sensors prior to the start of each trial. From this, the total movement in the arch was quantified.

### 3.2.3 Test 1: Bags over arch

The first test series conducted was designed to induce a deflection of the test arch section by positioning a mass over top of both the test arch section, and its entire 5-foot wide tributary area of tensioned fabric shell. This was accomplished by positioning the multi-chambered water storage system (MCWSS) such that the centre of the MCWSS was resting directly over the top of the test arch section. With the MCWSS positioned in this way, it extended approximately 2.5 feet on either side of the test arch section, and ensured that when the water was added to the chambers, the mass would act over the entire tributary area of the test section. The following picture (figure 8) shows the position of the MCWSS with respect to the test arch section.

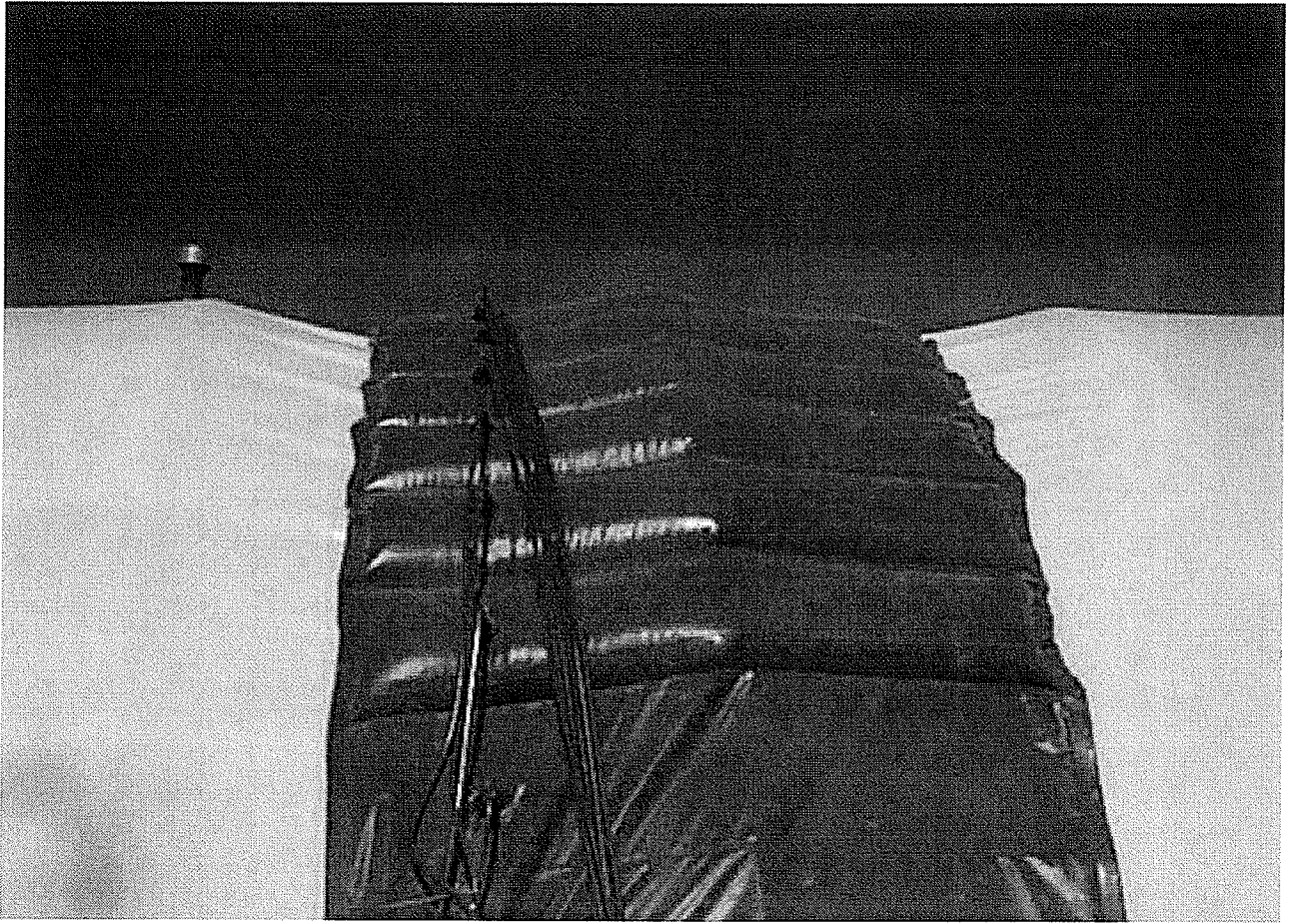


Figure 8: Position of the MCEWSS with respect to the test arch section  
(Gies, 2005)

With the MCWSS in position, the data acquisition system was manually started to record the output from the draw-wire displacement sensors at 15-second intervals.

With the data acquisition system recording the sensor data, the water supply to the central manifold system was turned on. Seventy-six litres (20 US gallons) of water, as measured by the volumetric flow meter, was sent to MCWSS one chamber at a time, starting from the centre of the test arch section, and gradually moving outwards. Filling of chambers was staggered from one side of the test arch to the other, to avoid an uneven application of mass.

Of the 24 individual chambers contained within the MCWSS, only 18 were used during the trials, 9 along each side of the test arch section. The final 3 chambers at either end of the MCWSS were not used because the slope of the test building roofline was in excess of 60° at the location of these chambers. An arch shaped building has a high degree of slope along much of the roof area. If a tangent line is taken at the peak of the roof, it would indicate a slope of zero degrees. This slope will increase in magnitude as tangent lines are taken increasingly farther away from the peak of the building. Because of the slope, sentence 31 of the NBC (1995) Commentary H states that the snow load may be reduced linearly moving out from the centre of the roof and towards the edge. The fabric covering the arch building can be considered to be a slippery surface, and therefore the snow load may be reduced from a full load at roof slopes of 15° or less, to zero load at 60° or more. The end-result of the slope factor will be that a significant area of the fabric-covered arch building will be considered to have zero snow load, as snow on the higher slope areas is assumed to fall off the side of the building.

With 76L (20 US gallons) of water added to each of the 18 chambers of the MCWSS, there was a total of 1368 L (360 US gallons) of water providing a uniform downward force of 1368kg (3000 pounds) over the test arch section.

After all the chambers had been filled, the water to the central manifold was shut off, and the test arch section was left in a hold period of 30 minutes with the load of 1368 kg (3000 pounds) remaining in place. This hold period allowed the full load applied by the water to deflect the test arch section to a constant degree for all trials.

Following the 30 minute hold period, the individual water valves attached at the central manifold for each water chamber on the MCWSS were opened, which allowed the water from each chamber to drain through an outlet on the central manifold. The MCWSS was left to drain for approximately 30 minutes, after which time the majority of the water had drained from all individual water chambers of the MCWSS. At this point, the data acquisition system was manually stopped, and the trial was completed. The central manifold and all individual water valves were left open overnight to allow any additional water left in the MCWSS to drain.

It was observed during the trials that the individual bags in the MCWSS were not able to completely drain away all of the water added during the tests. It was not possible to quantify the exact amount of water left in each of the chambers, and each trial started with the addition of 76L (20 U.S. gallons) of water that was in addition to the water still trapped within the bags. After the first trial using the MCWSS, it can be assumed that the volume of water remaining in each bag following each trial was similar. Therefore assuming that the total volume of water able to drain from the MCWSS was the same between each trial, all trials (with the exception of the first trial) would have used the same total volume of water.

The above process was repeated for an additional 2 trials to complete the load series for the bags over arch test arrangement.

### 3.2.4 Test 2: Bags beside arch

The second test series conducted was designed to induce a deflection of the test arch section by positioning a mass beside the test arch section, along the entire 5-foot wide section of tensioned fabric shell between the test arch and the adjacent arch. This was accomplished by positioning the centre of the MCWSS at approximately the midpoint in-between the test arch section and the adjacent arch. With the MCWSS positioned in this way, it covered the entire 5 foot width of canvas between the arches, and ensured that when the water was added to the chambers, the mass would act over the canvas adjacent to the test arch section, and not act directly on the arch itself. The following picture shows the position of the MCWSS with respect to the test arch section (Figure 9):

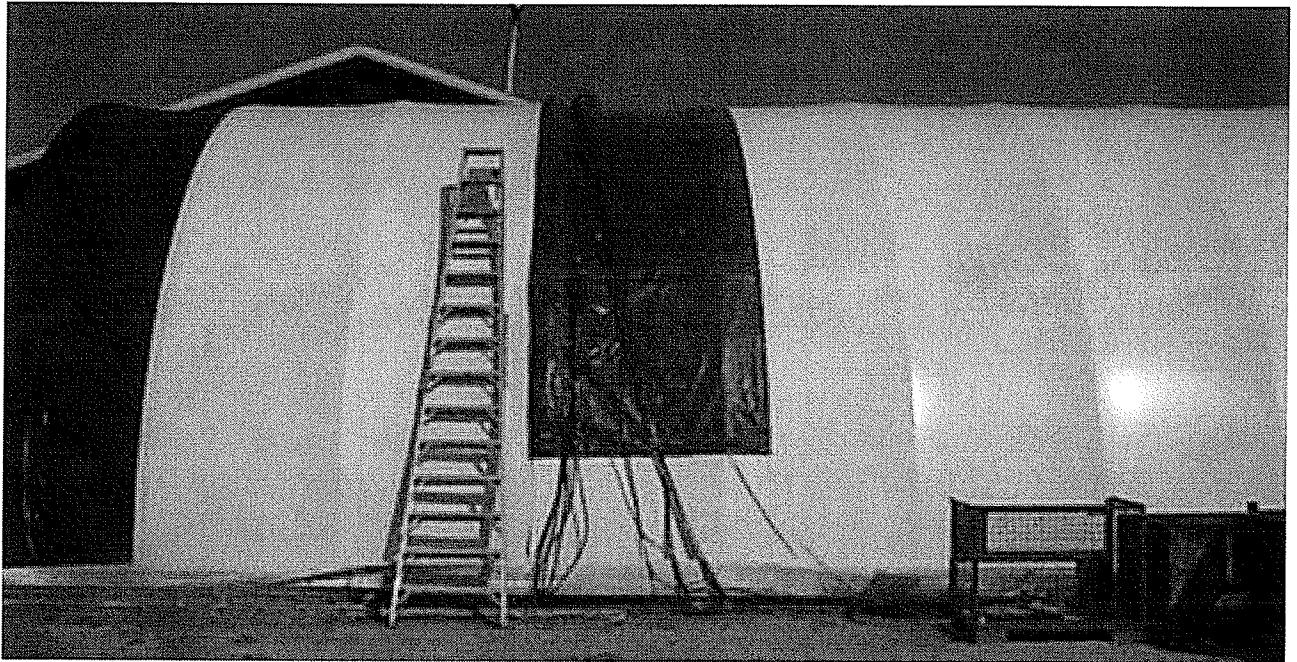


Figure 9: Position of the MCWSS with respect to the test arch section - Test 2  
(Gies, 2005)

With the MCWSS in position, the data acquisition system was manually started to record the output from the draw-wire displacement sensors at 15-second intervals.

With the data acquisition system recording the sensor data, the water supply to the central manifold system was turned on. Seventy-six litres (20 US gallons) of water, as measured by the volumetric flow meter, were sent to MCWSS one chamber at a time, starting from the centre of the test arch section, and gradually moving outwards. Filling of chambers was staggered from one side of the test arch to the other, to avoid an uneven application of mass.

As explained in section 2.2.3, of the 24 individual chambers contained within the MCWSS, only 18 were used during the trials, 9 along each side of the test arch section. The final 3 chambers at either end of the MCWSS were not used because the slope of the test building roofline was in excess of  $60^\circ$  at the location of these chambers.

With 76L (20 US gallons) of water added to each of the 18 chambers of the MCWSS, there was a total of 1368 L (360 US gallons) of water providing a uniform downward force of 1368kg (3000 pounds) over the 5-foot wide section of canvas adjacent to the test arch section.

After all the chambers had been filled, the water to the central manifold was shut off, and the test arch section was left in a hold period of 30 minutes with the load of 1368 kg (3000 pounds) remaining in place. This hold period allowed the full load applied by the water to deflect the test arch section to a constant degree for all trials.

Following the 30 minute hold period, the individual water valves attached at the central manifold for each water chamber on the MCWSS were opened, which allowed the water from each chamber to drain through an outlet on the central manifold. The MCWSS was

left to drain for approximately 30 minutes, after which time the majority of the water had drained from all individual water chambers of the MCWSS. At this point, the data acquisition system was manually stopped, and the trial was completed. The central manifold and all individual water valves were left open overnight to allow any additional water left in the MCWSS to drain.

The above process was repeated for an additional 2 trials to complete the load series for the bags beside arch test arrangement.

### 3.2.5 Test 3: Barrels under arch

The third and final test series conducted was designed to induce a deflection of the test arch section by positioning a mass that applied a load directly to the arch without involving its associated canvas tributary width. This was accomplished by using a separate method of mass application. Instead of using the MCWSS, a series of 50-gallon barrel pairs were attached to the underside of the arch section with chain. Fourteen, 50 U.S. gallon drum pairs were attached to the underside of the test arch section spaced two feet apart. The first barrel pair was attached to the test arch a distance of two linear feet away from the base of the building, and the remaining 13 barrel pairs attached at two-foot intervals along the remainder of the test arch. With the barrels spaced in such a manner, there was the same linear two-foot distance at both ends of the test arch, to coincide with the edge of the roofline where the slope was in excess of 60°, as explained in section 2.2.3. The barrel pair spacing maximized the amount of barrel pairs being used in load application, to coincide with the uniform loading of the MCWSS as closely as possible. When water was applied to these barrels, the downward force they provided would only act on the test arch member itself, without any interaction with the canvas.

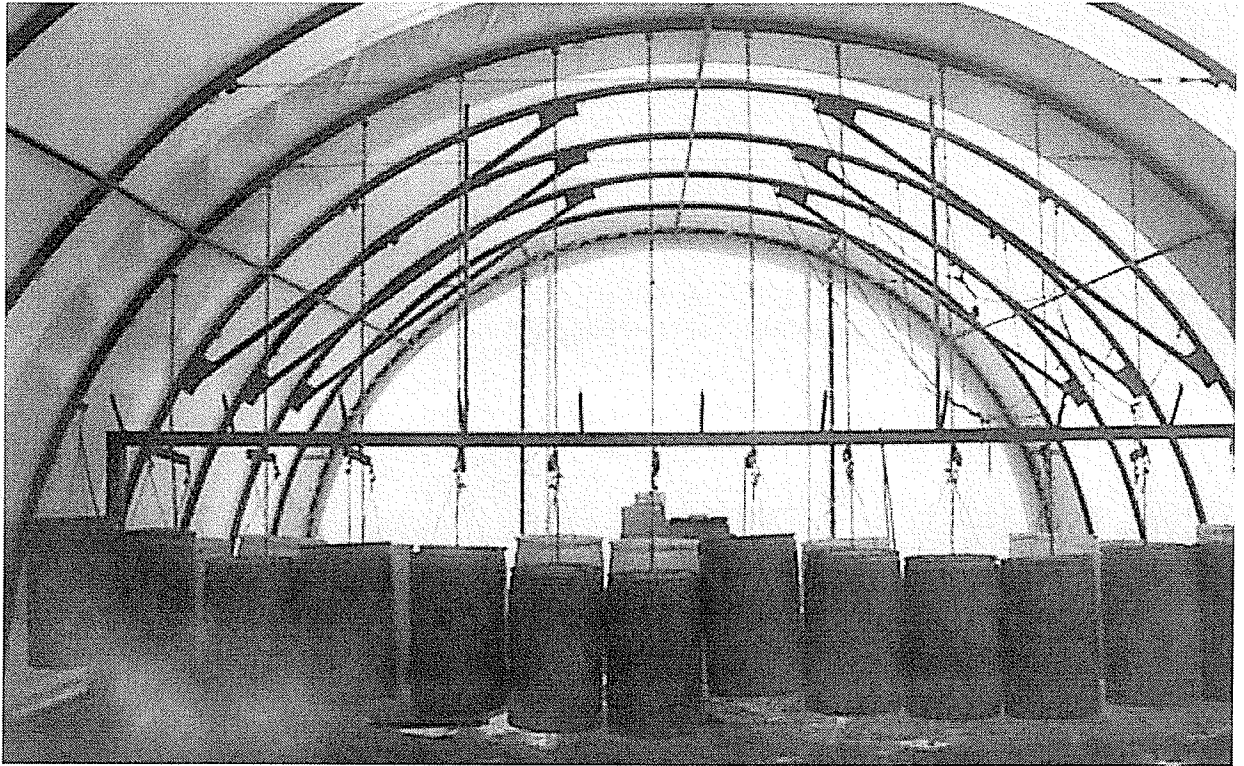


Figure 10: Barrels attached to the underside of the test arch section  
(Gies, 2005)

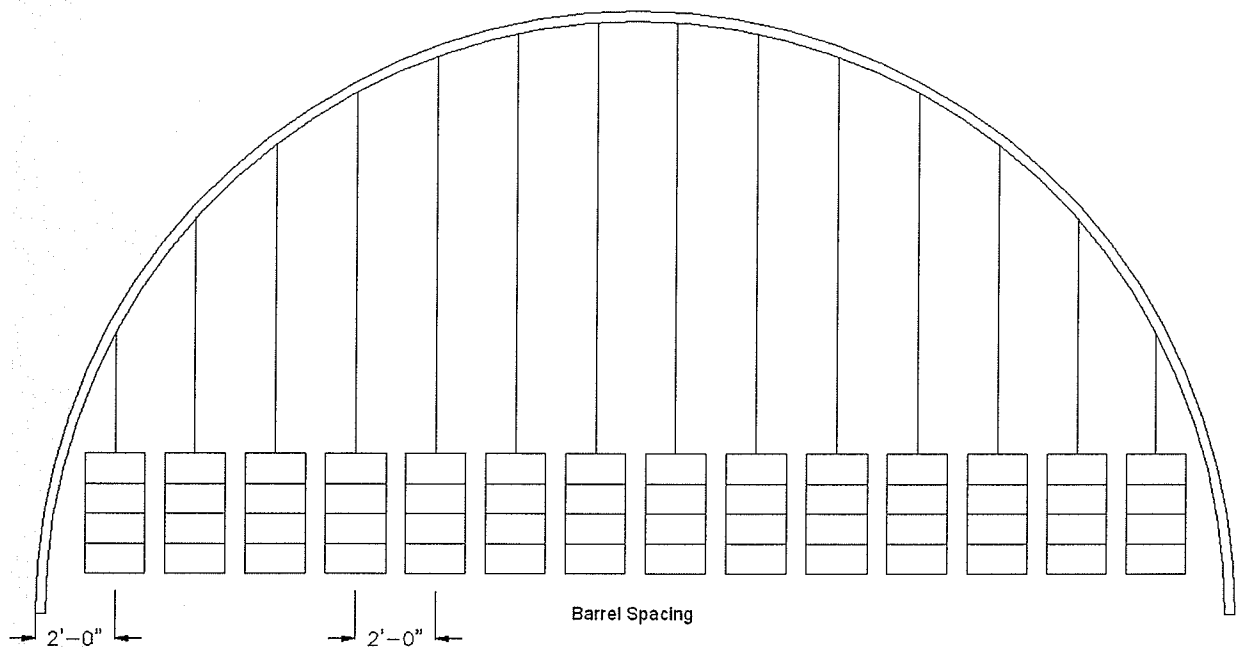


Figure 11: Position and spacing of barrels during testing  
(Gies, 2007)

To ensure the consistency between all tests, a downward force equal to that provided by the 360 gallons of water and the MCWSS had to be applied uniformly between all the 14 barrel pairs.

This downward force had to include the weight of each of the barrels (10 kg) the weight of the eight-foot length of chain (3.9 kg), and the weight of the barrel bracket (3.2 kg). Taking these weights into account, 68L (18 U.S. gallons) of water was required for each barrel pair during the tests to equal a total downward force of 1368L (360 U.S. gallons), or 3000 lb. The 68L of water required for each barrel pair would be divided equally between both barrels, 34L of water each.

With the barrels in position, the data acquisition system was manually started to record the output from the draw-wire displacement sensors at 15-second intervals.

With the data acquisition system recording the sensor data, the water supply to the central manifold system was turned on. Sixty-eight litres (18 US gallons) of water, as measured by the volumetric flow meter, was sent to each barrel pair, 34L of water per barrel, starting from the centre of the test arch section, and gradually moving outwards. Filling of barrels was done symmetrically about the centre-line of the test arch to the other, to avoid an uneven application of mass.

With 38L (18 U.S. gallons) of water added to each of the 14 barrel pairs, there was a combined total uniform downward force of 1368kg (3000 pounds) acting on the underside of the test arch section.

After all the barrels had been filled, the water to the central manifold was shut off, and the test arch section was left in a hold period of 30 minutes with the load of 1368 kg (3000 pounds) remaining in place. This hold period allowed the full load applied by the

water to deflect the test arch section to a constant degree for all trials.

Following the 30 minute hold period, the water in each barrel was manually emptied. At this point, the data acquisition system was manually stopped, and the trial was completed.

The above process was repeated for an additional 2 trials to complete the load series for the barrels under test arrangement.

## **4 RESULTS**

This research recorded the deflection of a steel test arch under three separate loading conditions. These three load conditions were devised to stress and induce a deflection in the test arch similar to the action of a uniform snow load acting on top of the building. Each load condition was tested in three separate trials, for a total of nine trials.

### **4.1 Results from Bags over Arch Test**

This test induced a deflection of the test arch section by positioning a mass over top of both the test arch section, and its entire 5-foot wide tributary area of tensioned fabric shell. Results from each trial were collected with the data acquisition system that was manually started prior to the application of water to the MCWSS. Data collected were in the form of output voltages from each of the 13 draw wire displacement sensors, and an additional channel to record the excitation voltage supplied to each displacement sensor. The data acquisition system was programmed to record the voltage readings from each of the 14 channels at 15 second intervals throughout each test, starting prior to the application of water to the MCWSS/barrels and ending after all the water had been drained and no further weight was acting on the test arch section.

The voltage data recorded during each test were converted into displacement data by using the calibration equations determined for each draw wire displacement sensor. The results from each of the three trials were combined to determine an average result for the Bags over Arch test. These data were then separated into a representative graph to display the average deflection of the entire arch vertically, a table to show the average deflection of the arch horizontally, and the average excitation voltage throughout the test.

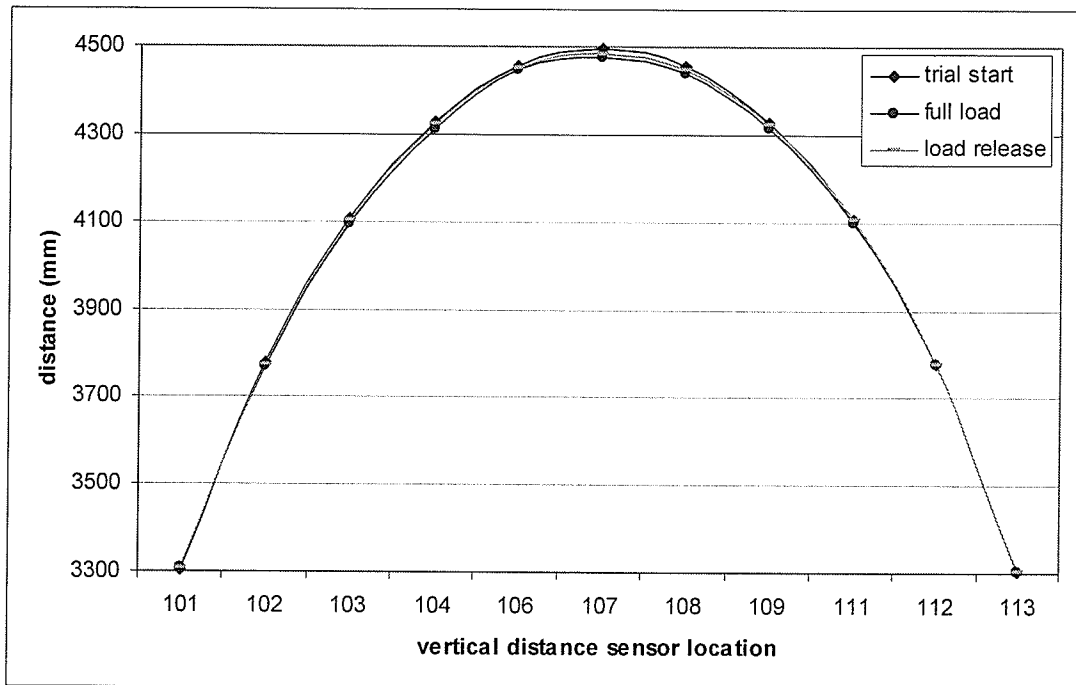


Figure 12: The average vertical deflection for each monitored location on the test arch at the trial start, trial full load, and load release as measured throughout each trial. Bags Over Arch (Gies, 2007)

Table 1: The average vertical deflection for sensors 104, 107 and 109 on the test arch as measured throughout each trial. Bags over Arch (Gies, 2007)

Time	Relative Change (mm)		
	sensor 104	sensor 107	Sensor 109
Trial Start	0.0	0.0	0.0
0h 30min	+0.2	-3.1	0.0
1h 00min	-5.0	-10.2	-4.3
1h 30 min	-12.8	-15.0	-10.3
2h 00 min	-15.0	-16.9	-12.6
2h 30 min	-16.4	-19.3	-13.0
3h 00 min	-16.9	-19.5	-13.4
3h 30 min	-14.9	-19.3	-12.6
Trial End	-4.7	-11.0	-4.3

Table 2: The average horizontal deflection for each displacement sensor on the test arch as measured throughout each trial. Bags Over Arch (Gies, 2007)

Time	sensor 105	sensor 110
	Relative Change (mm)	Relative Change (mm)
Trial Start	0.0	0.0
0h 30min	+0.1	0.0
1h 00min	+0.2	0.0
1h 30 min	+0.1	0.0
2h 00 min	0.0	-0.1
2h 30 min	0.0	-0.3
3h 00 min	-0.1	-0.3
3h 30 min	-0.1	-0.3
Trial End	-0.1	-0.2

The excitation voltage provided to each displacement sensor on the test arch was maintained at 10.0 VDC and measured throughout all trials, and the data are contained in Appendix A.

#### 4.2 Results from Bags Beside Arch Test

This test induced a deflection of the test arch section by positioning a mass beside the test arch section, along the entire 5-foot wide section of tensioned fabric shell between the test arch and the adjacent arch. Results from each trial were collected with the data acquisition system that was manually started prior to the application of water to the MCWSS. Data collected were in the form of output voltages from each of the 13 draw wire displacement sensors, and an additional channel to record the excitation voltage supplied to each displacement sensor. The data acquisition system was programmed to record the voltage readings from each of the 14 channels at 15 second intervals throughout each test, starting prior to the application of water to the

MCWSS/barrels and ending after all the water had been drained and no further weight was acting on the test arch section.

The voltage data recorded during the each test was converted into displacement data by using the calibration equations determined for each draw wire displacement sensor. The results from each of the three trials were combined to determine an average result for the Bags Beside Arch test. These data were then separated into a representative graph to display the average deflection of the entire arch vertically, a table to show the average deflection of the arch horizontally, and the average excitation voltage throughout the test.

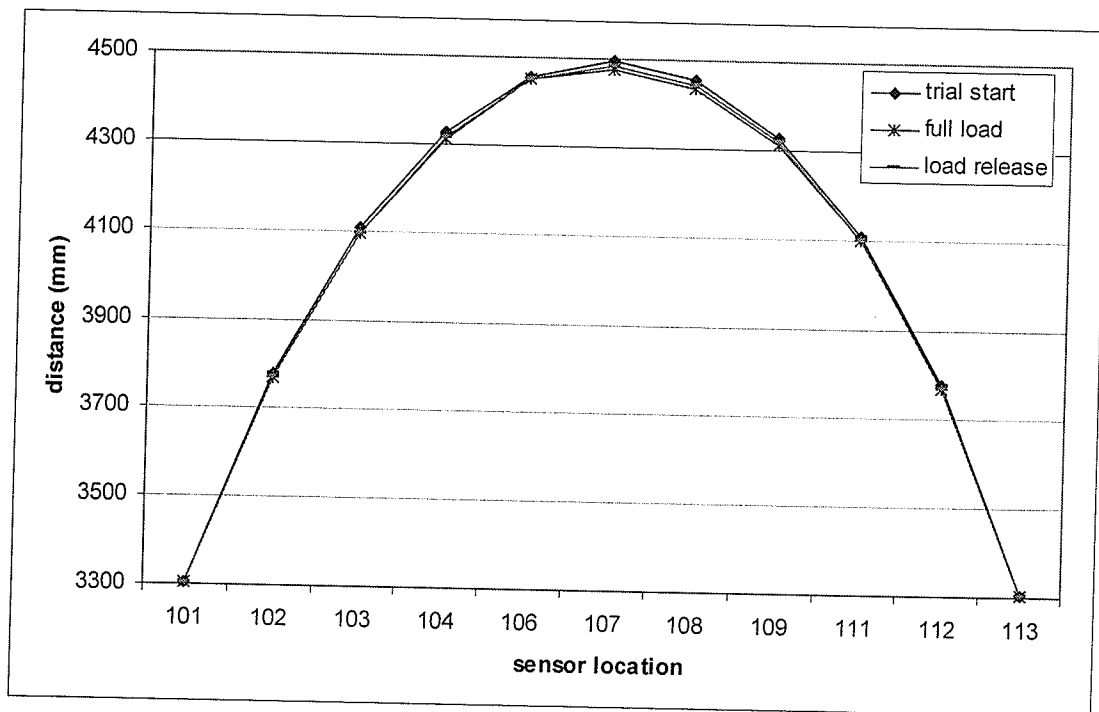


Figure 13: The average vertical deflection for each monitored location on the test arch at the trial start, trial full load, and load release as measured throughout each trial. Bags Beside Arch (Gies, 2007)

Table 3: The average vertical deflection for sensors 104, 107 and 109 on the test arch as measured throughout each trial. Bags Beside Arch (Gies, 2007)

Time	Relative Change (mm)		
	sensor 104	sensor 107	Sensor 109
Trial Start	0.0	0.0	0.0
0h 30min	-4.8	-11.6	-7.0
1h 00min	-12.9	-18.0	-13.8
1h 30 min	-18.2	-21.0	-16.6
2h 00 min	-18.6	-21.2	-16.7
2h 30 min	-18.4	-21.1	-16.7
Trial End	-11.3	-12.2	-10.1

Table 4: The average horizontal deflection for each displacement sensor on the test arch as measured throughout each trial. Bags Beside Arch (Gies, 2007)

Time	sensor 105	sensor 110
	Relative Change (mm)	Relative Change (mm)
Trial Start	0.0	0.0
0h 30min	0.0	+0.1
1h 00min	0.0	+0.1
1h 30 min	0.0	-0.4
2h 00 min	0.0	-0.8
2h 30 min	0.0	-0.9
Trial End	0.0	-0.9

The excitation voltage provided to each displacement sensor on the test arch was maintained at 10.0 VDC and measured throughout all trials, and the data is contained in Appendix A.

### **4.3 Results from Barrels Under Arch Test**

This test induced a deflection of the test arch section by positioning a mass that applied a load directly to the arch without involving its associated canvas tributary width. Results from each trial were collected with the data acquisition system that was manually started prior to the application of water to the MCWSS. Data collected were in the form of output voltages from each of the 13 draw wire displacement sensors, and an additional channel to record the excitation voltage supplied to each displacement sensor. The data acquisition system was programmed to record the voltage readings from each of the 14 channels at 15 second intervals throughout each test, starting prior to the application of water to the MCWSS/barrels and ending after all the water had been drained and no further weight was acting on the test arch section.

The voltage data recorded during the each test was converted into displacement data by using the calibration equations determined for each draw wire displacement sensor. The results from each of the three trials were combined to determine an average result for the Barrels Under Arch test. These data were then separated into a representative graph to display the average deflection of the entire arch vertically, a table to show the average deflection of the arch horizontally, and the average excitation voltage throughout the test.

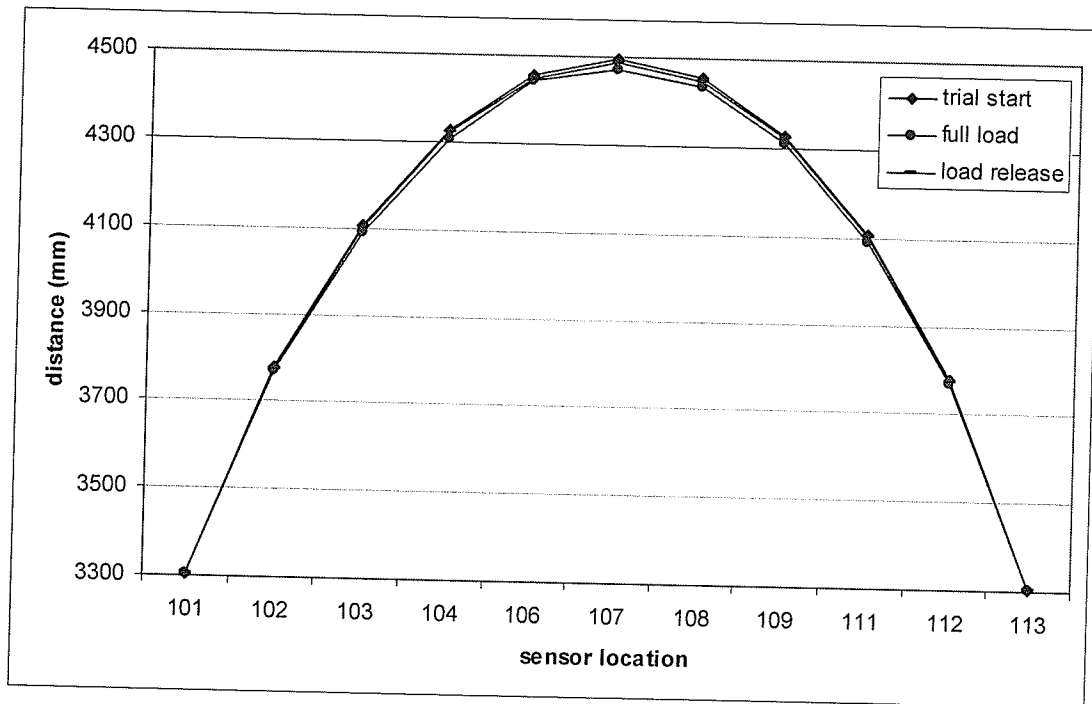


Figure 14: The average vertical deflection for each monitored location on the test arch at the trial start, trial full load, and load release as measured throughout each trial. Barrels Under Arch (Gies, 2007)

Table 5: The average vertical deflection for sensors 104, 107 and 109 on the test arch as measured throughout each trial. Barrels Under Arch (Gies, 2007)

Time	Relative Change (mm)		
	sensor 104	sensor 107	Sensor 109
Trial Start	0.0	0.0	0.0
0h 30min	-5.5	-9.9	-6.2
1h 00min	-13.7	-19.7	-16.6
1h 30 min	-18.0	-21.7	-18.0
2h 00 min	-18.9	-22.1	-18.0
2h 30 min	-19.5	-22.4	-17.7
3h 00 min	-16.3	-21.0	-13.6
Trial End	-6.2	-9.9	-4.2

Table 6: The average horizontal deflection for each displacement sensor on the test arch as measured throughout each trial. Barrels Under Arch (Gies, 2007)

Time	sensor 105	sensor 110
	Relative Change (mm)	Relative Change (mm)
Trial Start	0.0	0.0
0h 30min	-2.9	-1.8
1h 00min	-2.9	-2.1
1h 30 min	-2.9	-2.3
2h 00 min	-2.9	-2.5
2h 30 min	-3.0	-2.8
3h 00 min	-3.4	-3.0
Trial End	-3.5	-3.4

The excitation voltage provided to each displacement sensor on the test arch was maintained at 10.0 VDC and measured throughout all trials, and the data is contained in Appendix A.

## **5 DISCUSSION**

This discussion is based on the analysis of the data captured during the three (3) different test methods comprising of a total of nine (9) total trials. The data analysis discussed in this section was focused on specific monitored locations, to examine similar data points in each test and trial for comparison purposes. The data files in their entirety for each trial are contained in Appendix A.

### **5.1 Vertical Deflection**

For the purposes of comparison, three (3) deflection sensors were chosen to compare the vertical deflection of the test arch throughout the different tests. The sensors were chosen based on the amount of deflection experienced during the trials to maximise the visual representation of the results in this discussion. The results of each trial showed that the vertical deflection sensors located at or near the peak of the arch consistently deflected to the greatest distance. Accordingly, the vertical deflection sensor positioned at the test arch peak, sensor 107 was used, along with sensors 104 and 109. Vertical deflection sensors 104 and 109 were both positioned a distance of 610mm (4 ft) on either side of sensor 107 (refer to Figure 6).

### 5.1.1 Discussion Bags over Arch Test

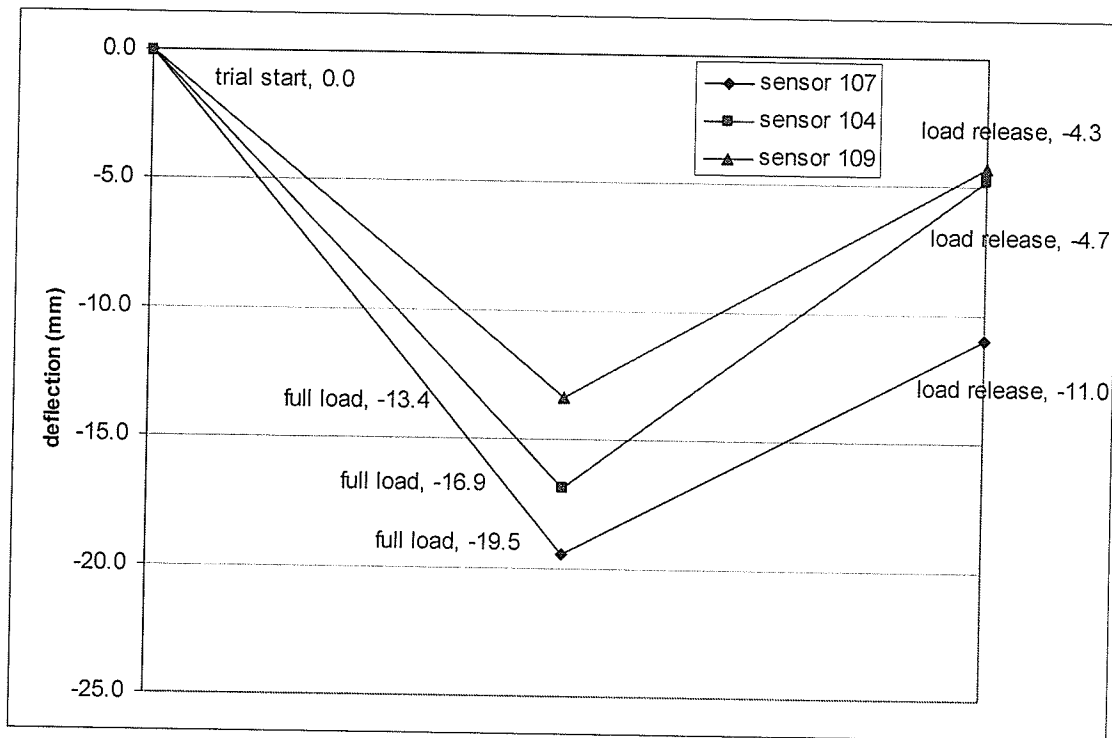


Figure 15: The deflection during Bags Over Arch test averaged over 3 trials for vertical displacement sensors 104, 107 and 109 on the test arch at the trial start, trial full load, and load release (Gies, 2007)

Figure 15 indicates that the application of a 3000 pound load, uniformly distributed directly over top of the effective length of the test arch induced a measurable deflection, as noted on the graph. The data shows that sensor 107 located at the peak of the test arch, deflected 5.1 and 2.4 mm further when compared with sensors 104 and 109 respectively. The slopes of the graph indicate the rate at which the deflection occurred during each trial. The graph shows that Sensor 107 is subjected to a faster rate of deflection compared to the other sensors as evidenced by the steeper slope associated with its deflection downwards. This coincides with the pattern of load application to the

test arch, where the chambers of the MCWSS at the peak of the test arch were filled first. The graph indicates that none of the sensors rebounded back to their starting point of 0.0mm within the trial period. The slopes in the graph highlight a distinction between the load application rate and load release rate in the Bags Over Arch trials. The slopes from start to full load are more steep and pronounced than the slopes from full load to load release. This shows that the test set-up for the Bags Over Arch trials allowed for load to be applied faster than it could be released. These data also correspond with the observation made during the testing that some water remained in the MCWSS after it stopped draining following the release of the 3000 pound water load.

### 5.1.2 Discussion Bags Beside Arch Test

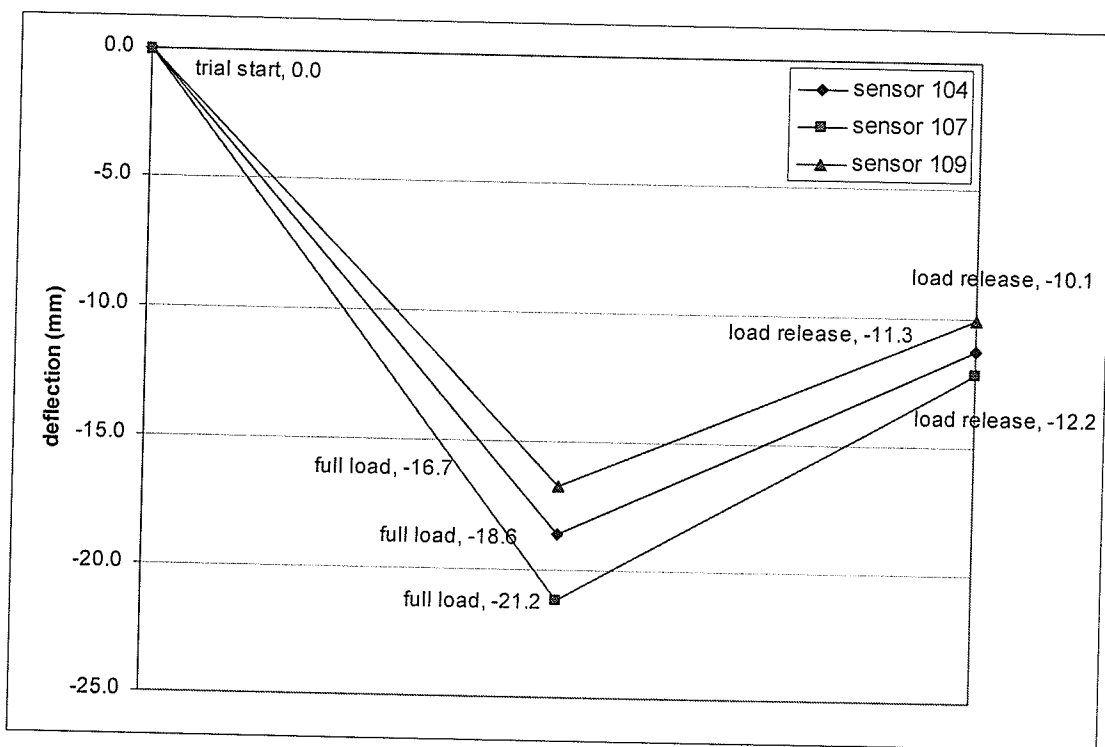


Figure 16: The deflection during Bags Beside Arch test averaged over 3 trials for vertical displacement sensors 104, 107 and 109 on the test arch at the trial start, trial full load, and load release (Gies, 2007)

Figure 16 indicates that the application of a 3000 pound load, uniformly distributed along the entire effective length of the 5-foot wide section of tensioned fabric shell beside the test arch induced a measurable deflection, as noted on the graph. The data shows that sensor 107 located at the peak of the test arch, deflected 4.5 and 2.6 mm further when compared to sensors 104 and 109 respectively. The slopes of the graph indicate the rate at which the deflection occurred during each trial. The graph shows that Sensor 107 was subjected to a faster rate of deflection compared to the other sensors as evidenced by the steeper slope associated with its deflection downwards. This coincides with the pattern of load application to the test arch, where the chambers of the MCWSS at the peak of the test arch were filled first. The graph indicates that none of the sensors rebounded back to their starting point of 0.0mm within the trial period. The slopes in the graph highlight a distinction between the load application rate and load release rate in the Bags Beside Arch trials. The slopes from start to full load are more steep and pronounced than the slopes from full load to load release. This shows that the test set-up for the Bags Beside Arch trials allowed for load to be applied faster than it could be released. This data also correlates with the observation made during the testing that some water remained in the MCWSS after it stopped draining following the release of the 3000 pound water load.

### 5.1.3 Discussion Barrels Under Arch Test

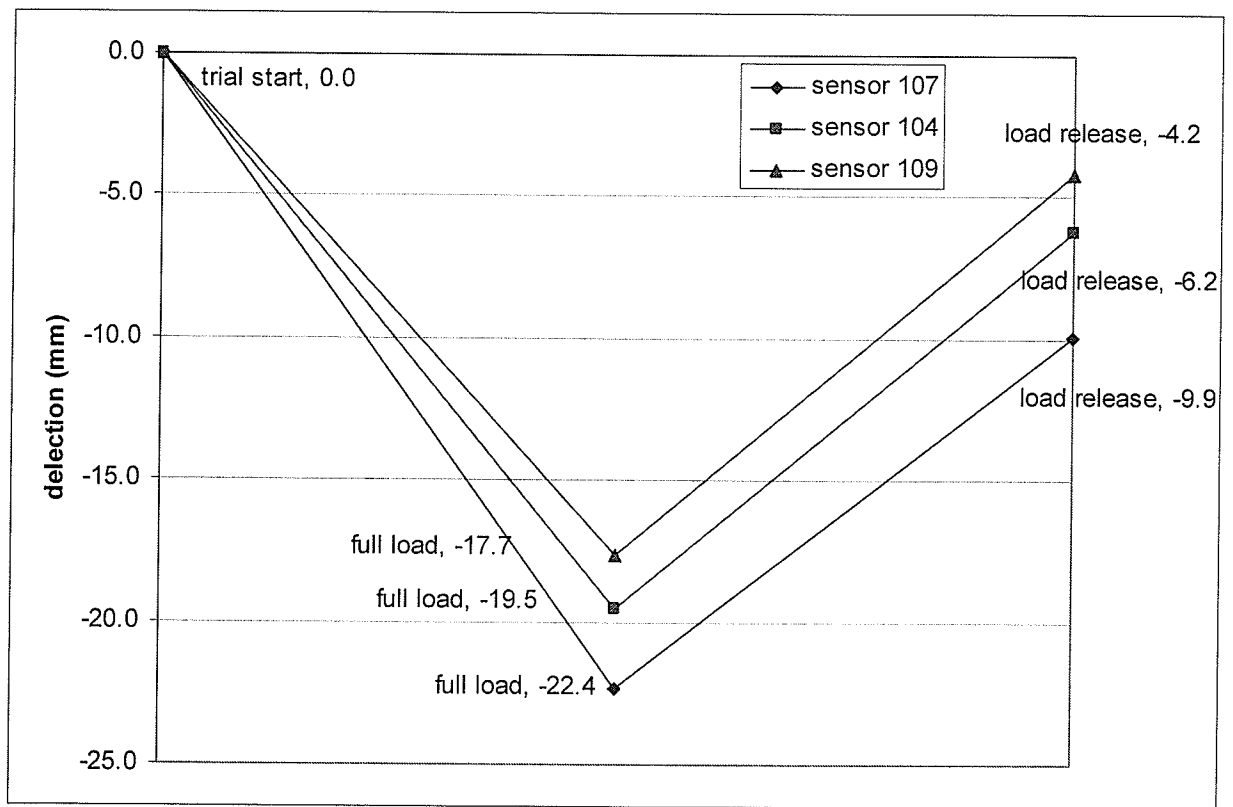


Figure 17: The deflection during Barrels Under Arch test averaged over 3 trials for vertical displacement sensors 104, 107 and 109 on the test arch at the trial start, trial full load, and load release (Gies, 2007)

Figure 17 indicates that the application of a 3000 pound load, uniformly distributed among a series of barrels positioned directly beneath the effective length of the test arch induced a measurable deflection, as noted on the graph. The data show that sensor 107 located at the peak of the test arch, deflected 4.7 and 2.9 mm further when compared to sensors 104 and 109 respectively. The slopes of the graph indicate the rate in which the deflection occurred during each trial. The graph shows that all of the sensors react similarly to the load application and to the load release. These data coincide

with the test procedure, as the barrels were manually drained of water following each test, and unlike the MCWSS, it could be confirmed that all load had been removed from the test arch after each trial. The graph indicates that none of the sensors rebounded back to their starting point of 0.0mm within the trial period. The lack of complete rebound in the test arch captured in the results may be partially due to the stoppage in data collection immediately following the release of the load on the test arch. The stoppage of data collection following the load release in each trial meant that the subsequent rebound in the test arch was not completely captured in each data file.

Figures 15 through 17 show a consistent amount of deflection captured by the vertical displacement sensors through each of the three different tests. The most obvious differences between the Figures are in the relative slopes between the data points. These relative slopes show the effectiveness of the load application in all trials, and the differences in the effectiveness and speed at which the load was removed from the test arch, load release from the MCWSS clearly requires greater time when compared to that of the barrels.

#### 5.1.4 Computer Aided Modeling Analysis Discussion

For an additional point of vertical deflection comparison, a structural analysis software program was utilized to compare the predicted deflection of a simulated test arch section against the results of the three different, full scale tests completed as part of this research. To model and analyze a simulated test arch section, the structural analysis program RISA-3D was used to draw the model, apply simulated loads, and analyse the resulting vertical deflections. The test arch section created in RISA-3D was drawn to scale, with the simulation analysed using the same materials and dimensions as the test

arch section used throughout each of the tests procedures. To load the simulated test arch section as closely as possible to the loads applied using the barrels and the MCWSS, the total water load of 1368 kg (3000 pounds) was divided into 27, 50kg (111 pound) point loads applied to the top of the test arch section at 300 mm (1-foot) intervals. The point loads started at the peak of the arch, and extended 13 feet on either side, such that the last two feet of arch surface on both side of the arch remained unloaded, following the three test procedures.

Figure 18 below shows the simulated test arch as represented by RISA-3D.

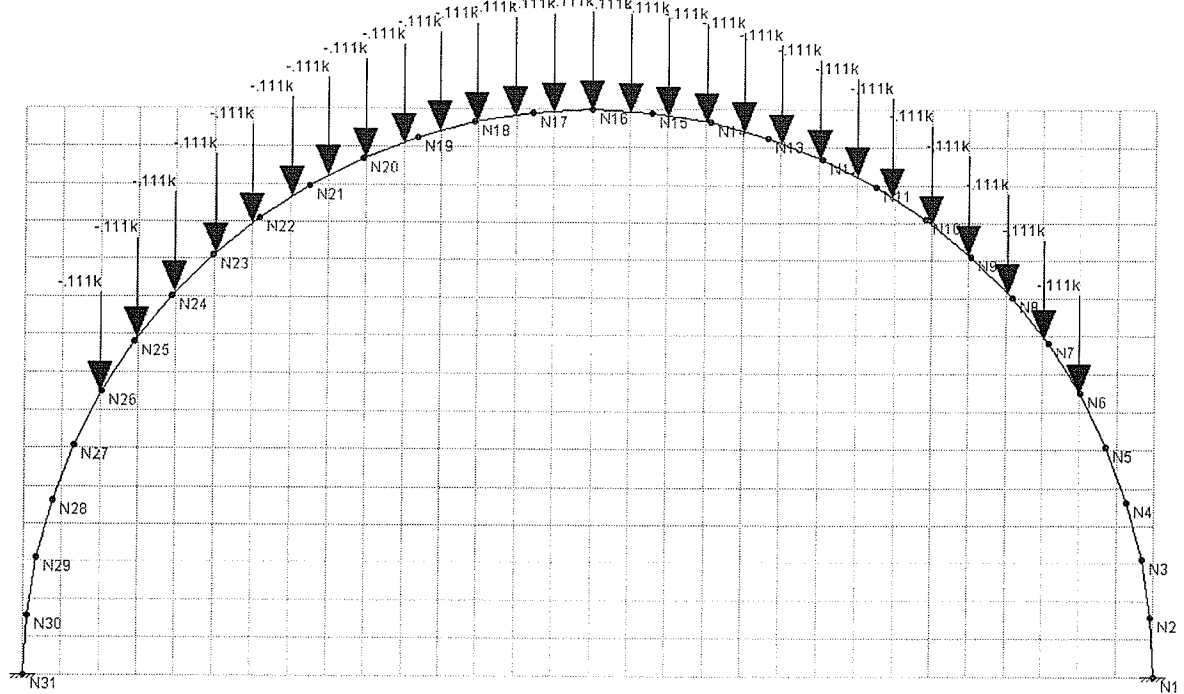


Figure 18: Simulated test arch section analysed by RISA-3D (Gies 2007)

Nodes on the simulated test arch section were chosen at locations as close as possible to the locations of sensors 104, 107 and 109 used during the 3 test procedures for comparison purposes. The nodes used were N19, N16, and N13 to represent sensor 104, 107 and 109 respectively.

Table 7: The average vertical deflection for computer model nodes N13, N16 and N19 on the simulated test arch as analysed and predicted by RISA-3D.  
(Gies, 2007)

Time	Relative Change (mm)		
	Node 19	Node 16	Node 13
Trial Start	0.0	0.0	0.0
Full Load	-45.2	-64.7	-45.2
Load Release	0.0	0.0	0.0

Table 7 indicates a large difference in the deflection measured during the three test procedures and the deflection that is predicted using a structural analysis program. The deflections recorded for node 19 and 13 are seen to be the same since the simulated test arch in Risa3D ensures that the loading is symmetrical about the centreline of the arch. The three test procedures completed for this project in the field could not match the precision of the analysis software, or ensure the exact symmetrical loading of the test arch. As a result there is a high degree of difference between the results of the software analysis, and the three test procedures. This difference is highlighted in Table 8 below, where the test procedures all averaged between 61% and 68% less maximum deflection during the tests, as compared to the Risa3D deflection prediction.

Table 8: A comparison of the average maximum vertical deflections recorded during the test procedures and with those predicted by Risa3D (Gies, 2007)

Test Procedure	Measured deflection (mm)		Risa3D predicted deflection (mm)		Percent difference	Average percent difference
	sensor		node			
Bag over arch test	104	-16.4	N19	-45.2	64%	68%
	107	-19.5	N16	-64.7	70%	
	109	-13.4	N13	-45.2	70%	
Bag beside arch test	104	-18.6	N19	-45.2	59%	63%
	107	-21.2	N16	-64.7	67%	
	109	-16.7	N13	-45.2	63%	
Barrels under arch test	104	-17.7	N19	-45.2	61%	61%
	107	-22.4	N16	-64.7	65%	
	109	-19.5	N13	-45.2	57%	

The deflections predicted by the RISA3D software are closest to the barrels under arch test procedure. This is because the methods of applying the load to the arch itself are similar between both tests. In both tests the load is applied directly to the test arch section in the Y-direction without any load being transferred through the tensioned fabric membrane. What can be inferred from this is that the major difference between the results from the barrels under arch test, and the simulated test using the RISA3D software is how the tensioned fabric membrane interacts with the test arch member as load is applied. It is postulated that the variance in results may be attributed to the tensioned fabric shell acting to stiffen the entire structure, preventing the deflection of the test arch member from reaching the levels predicted by the RISA3D software.

## 5.2 Horizontal Deflection

Sensors 105 and 110 on the test arch were positioned to measure any horizontal deflection in the test arch that was induced with the load application during each of the nine trials. Horizontal deflection sensors 105 and 110 were both positioned a distance of 610mm (4 ft) on either side of sensor 107 (refer to Figure 6).

In section 3, the average horizontal deflection data for the three trials captured during the trials was presented in tabular form; Table 1 for the Bags Over Arch test, Table 2 for the Bags Beside Arch test, and Table 3 for the Barrels Under Arch test. For comparison purposes, the tabulated data for each test was put in graphical form to observe the differences in the average horizontal deflection data recorded in each test. Figure 19 and Figure 20 show the graphical representation of the horizontal deflection data recorded at sensors 105 and 110 respectively, at the trial start, full load and load release.

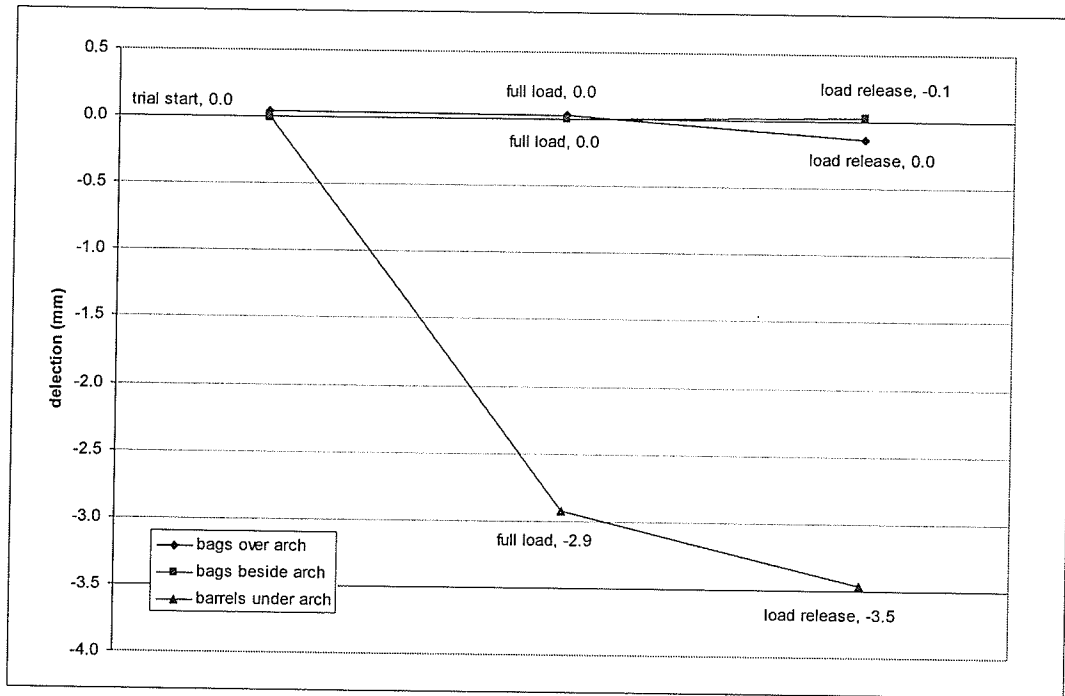


Figure 19: The average deflection over all tests for horizontal displacement sensor 105 at the trial start, trial full load, and load release (Gies, 2007)

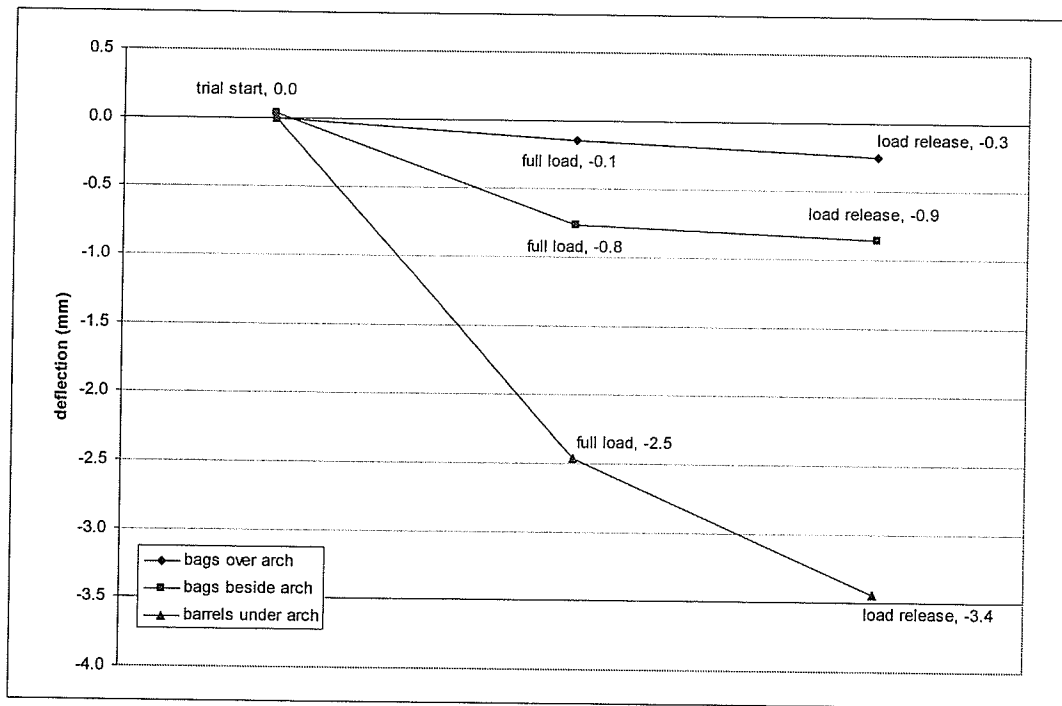


Figure 20: The average deflection over all tests for horizontal displacement sensor 110 at the trial start, trial full load, and load release (Gies, 2007)

Figure 19 shows that the horizontal deflection sensor 105 deflected 0.1mm, 0.0mm, and 3.5mm on average for the Bags Over Arch, Bags Beside Arch and Barrels Under Arch tests, respectively. The graph also shows that there is no discernable change in the deflection captured at the sensor at the different stages of each trial. Unlike the vertical deflection sensors, it is not possible to tell by looking at the graph when load is applied and released. The average deflection distance recorded at 105 was extremely small in the Bags Over Arch and Barrels Under Arch tests, and no deflection was captured during the entire Bags Beside Arch test.

Figure 20 shows that the horizontal deflection sensor 110 deflected 0.3mm, 0.9mm, and 3.4mm on average for the Bags Over Arch, Bags Beside Arch and Barrels Under Arch tests, respectively. The graph also shows that there is no discernable change in the deflection captured at the sensor at the different stages of each trial. Similar to Figure 19, it is not possible to tell by looking at the graph when load is applied and released and the average deflection distance recorded at 105 was extremely small over all tests completed. The inconsistent data captured by the horizontal displacement sensors indicates that none of the tests completed on the test arch induced any measurable lateral deflection.

### **5.3 Co-efficient of Lateral Stability**

To establish a co-efficient that relates the behaviour of the interaction between the steel-arch and tensioned fabric membrane, it is necessary to compare the average deflection results from each test procedure. The results will be compared at the peak of the test arch section, sensor 107, because this was the area that consistently experienced the largest total deflection distance in each trial for the purposes of this report.

The deflection data from the Barrels Under Arch test procedure will be used as a the basis point from which to determine the co-efficient of lateral stability, as this test did not apply the load to any part of the tensioned fabric membrane, only the test arch section itself. Therefore the differences between the results would presumably be caused by the transfer of the vertical load through the tensioned fabric shell, and into the test arch section.

Table 9: Co-efficient of lateral stability based on the barrels under arch test results (Gies, 2007)

Test Procedure	deflection at peak (mm)	deflection at peak barrels under arch test	Co-efficient of lateral stability	Corresponding percentage
Bag over arch test	19.5	22.4	0.87	13%
Bag beside arch test	21.2	22.4	0.95	5%

The numbers in Table 9 indicate that at the peak of the arch, the tensioned fabric membrane reduced the deflection by between 5 and 13%. However the tensioned fabric membrane does not only interact with the structure in terms of transferring load down to the steel arch, it also must play a role in stiffening the entire structure, preventing the steel arch members from bowing outwards, and therefore minimising further vertical deflection along the steel arch.

For a more accurate prediction of a co-efficient of lateral stability, it would be beneficial to have deflection data from a test arch section that was tested without a tensioned fabric shell. These results would have provided a more accurate basis point to determine the co-efficient of lateral stability, as compared to the barrels under arch test results.

In the absence of experimentally derived deflection data for a test arch section without a tensioned fabric shell, the results from the RISA3D software analysis could be used to predict a more accurate co-efficient of lateral stability. Using this software data would only be a prediction, as the deflection values used were not experimentally derived in the same manner as the test procedures. As discussed previously, the RISA3D software results will only be compared against the barrels under arch data.

Table 10: Co-efficient of lateral stability using the barrels under arch test and the RISA3D software peak of arch deflection data.

(Gies, 2007)

deflection at peak (mm)		Co-efficient of lateral stability	Corresponding percentage
Barrels under arch	RISA3D software		
22.4	64.7	0.35	65%

The numbers in Table 10 indicate that when using the deflection of the test arch section predicted by the RISA3D software at the peak of the arch, the tensioned fabric membrane reduced the deflection by 65%.

## 6 CONCLUSION

The behaviour of a full-scale fabric covered steel arch was studied under three separate loading conditions. These loading scenarios were the water bags over arch, water bags beside arch and loaded barrels suspended under the arch. For each test procedure three separate trials were completed. Deflection data in both vertical and horizontal out-of-plane directions was collected and analysed. In addition to the three test procedures, a structural analysis computer software program was used to simulate the test conditions to provide an additional set of comparison data.

The averaged results from the three different loading conditions indicate that there are small differences between the vertical deflections experienced by the arch when it is loaded from directly over top of the arch and beside the arch using the tensioned fabric membrane, and when it was loaded from the bottom of the test member itself, without the direct interaction of the tensioned fabric membrane.

The data recorded from the test procedures showed a maximum deflection at the peak of the arch as 19.5 mm for the Bags Over Arch test, 21.2 mm for the Bags Beside Arch test, and 22.4 mm for the Barrels Under Arch test.

These deflection numbers for the peak of the test arch differed greatly from the deflection predicted for the peak of the arch by the RISA3D software where the deflection was 64.7 mm at the peak of a simulated test arch loaded under similar conditions to the test procedures.

This large difference may be attributed to the lack of fabric cladding applied to the arch simulated using the RISA3D structural analysis software. The test arch used for the three test procedures was clad with a tensioned fabric membrane that may have helped to

stiffen the test arch section, preventing its deflection outwards and downwards, to the deflections that were predicted by the RISA3D structural analysis software.

The results collected for the horizontal deflection were extremely small in terms of linear translation, and inconsistent between both test procedures and individual trials. As a result, no behaviour of the test arch can be inferred from the test procedures in terms of horizontal deflections.

When using the barrels under arch test deflections as a basis point for determining the co-efficient of lateral stability, it was found that the tensioned fabric membrane reduced the deflection at the peak of test arch section by 0.95 and 0.87 (or 5 and 13%) when comparing the results against the bags over arch and bags beside arch test procedures respectively.

All three of the test procedures were influenced by the tensioned fabric membrane that formed the cladding of the structure used to perform the experiments. Therefore to determine a more accurate value for the co-efficient of lateral stability, it is necessary to compare the data collected as part of this research against data collected from a test arch section that was not clad with a tensioned fabric membrane.

In the absence of experimentally derived data, the simulated test arch section analysed with the RISA3D software could be used as a benchmark for the behaviour of a typical arch section without the interaction of a tensioned fabric membrane, and these results could be compared against the data collected with the barrels under arch tests. The results from these tests could be compared because the application of load on the test arch section is similar between the barrels under arch test and the simulated loading completed using the RISA3D software. Using the deflection at the peak of the arch, the

co-efficient of lateral stability between the deflection recorded with the barrels under arch test and the deflection predicted with the RISA3D software could be taken as 0.35 for the peak of the arch, meaning that the tensioned fabric membrane is preventing 65% of the deflection that a similarly loaded test arch section would experience when tested on its own.

This co-efficient can only be inferred at this point, as the deflection value for one set of the comparison data is based on simulated and not experimentally derived data.

## **7 RECOMMENDATIONS FOR FURTHER STUDY**

It would be beneficial to determine the interaction between the tension of the outer membrane and the overall stability of tensioned fabric buildings for further study. A possible experiment could correlate the exterior wind pressures with loads recorded at load cells installed at strapping points within the tensioned membrane. This experiment could also look further into how a tensioned membrane reacts to outside forces that cause a loss of its anticlastic surface (internal stress reversal). With the loss of the anticlastic surface, it would be beneficial to study the effects of this internal stress reversal and the resultant forces on the main structural members of the building.

It is also recommended to test a test-arch section without the tensioned fabric membrane to determine the baseline deflection results to compare against test procedures completed with the interaction of the membrane. These data could also be used as a comparison point for data derived from structural analysis software applications.

## 8 REFERENCES

1. HiQual Manufacturing Ltd. 2002. Portable Quonset Building Model PQ3045 Owner's Manual. Winnipeg, MB.
2. Huntington, C. G. 2004. *The Tensioned Fabric Roof*. Reston, VA: ASCE Press.
3. Leonard, J. W. 1988. *Tension Structures Behaviour and Analysis*. Toronto, ON: McGraw-Gill Book Company.
4. National Research Council of Canada. 2005. *National Building Code of Canada 2005*. Ottawa, ON.
5. National Research Council of Canada. 2005. *User's Guide – NBC 2005 Structural Commentaries (Part 4 of Division B)*. Ottawa, ON.
6. RISA Technologies Software. 2003. *Rapid Interactive Structural Analysis – 3-Dimensional Version 5.0*. Foothill Ranch, California.
7. Schierle, G. G. 1968. *Lightweight Tension Structures*. Berkeley, CA: Department of Architecture, University of California.
8. Shaeffer, R. E. 1996. *Task Committee on Tensioned Fabric Structures*. New York, NY: ASCE.
9. Trebilcock, P. and M. Lawson. 2004. *Architectural Design in Steel*. New York, NY: Spoon Press Taylor and Francis Group.
10. Valeria, J. M. 1985. *Architectural Fabric Structures: The Use of Tensioned Fabric Structures by Federal Agencies*. Washington, D.C.: National Academy Press.

## 9 BIBLIOGRAPHY

1. Carradine, D.M. and R.H. Plaut. 1998. Experiments on the response of arch supported membrane shelters to snow and wind loading. *International Journal of Space Structures*, 13: 197-202.
2. Clarke, M.J. and G.J Hancock. 1995. Tests and nonlinear analyses of small-scale stressed-arch frames. *Journal of Structural Engineering*, 121: 187-200.
3. Dopker, B., K.K. Choi and R.L Benedict. 1988. Shape design sensitivity analysis of structures containing arches. *Computers and Structures*, 28(1): 1-13.
4. Khan, U.H., H.S. Mitri and D. Jones. 1996. Full scale testing of steel arch tunnel supports. *International Journal of Rock Mechanics Mining Sciences and Geomechanics Abstracts*, 33(3): 219-232.
5. Krishna, P. 2001. Tension roofs and bridges. *Journal of Constructional Steel Research*, 57: 1123-1140.
6. Molloy, S.J., R.H. Plaut and J.Y. Kim. 1999. Behaviour of pair of leaning arch shells under snow and wind loading. *Journal of Engineering Mechanics*, 125(6): 663-667.
7. Pi, Y.L. and N.S. Trahair. 1996. In-plane inelastic buckling and strengths of steel arches. *Journal of Structural Engineering*, 122: 734-747.
8. Pi, Y.L. and N.S. Trahair. 1999. In-plane buckling and design of steel arches. *Journal of Structural Engineering*, 125: 1291-1298.
9. Pi, Y.L. and N.S. Trahair. 1999. Out-of-plane inelastic buckling and strength of steel arches. *Journal of Structural Engineering*, 124: 174-183
10. Plaut, R.H., J.K.S. Goh, M. Kigudde and D.C. Hammond. 2000. Shell analysis of an inflatable arch subjected to snow and wind loading. *International Journal of Solids and Structures*, 37: 4275-4288.

11. Sakimoto, T. and S. Komatsu. 1983. Ultimate strength formula for steel arches. *Journal of Structural Engineering*, 109: 613-627.
12. Tobiasson, W. 1999. Snow loads on gable roofs. *Journal of Structural Engineering*, 125: 470-473.
13. Turnbull, J.E. and D.I. Masse. 1988. Strength and deformation of nailed wood gambrel roof arches. *Canadian Agricultural Engineering*, 30(1): 157-163.

## **10 APPENDIX**

Refer to attached CD-ROM for data files.